

1   **Coupled eco-hydrology and biogeochemistry algorithms enable simulation of water table**  
2   **depth effects on boreal peatland net CO<sub>2</sub> exchange**

3

4   Mohammad Mezbahuddin\*<sup>1,2</sup>, Robert F. Grant<sup>2</sup>, and Lawrence B. Flanagan<sup>3</sup>

5

6   <sup>1</sup>*Environmental Stewardship Branch, Alberta Agriculture and Forestry, Edmonton, AB, Canada*

7   <sup>2</sup>*Department of Renewable Resources, University of Alberta, Edmonton, AB, Canada*

8   <sup>3</sup>*Department of Biological Sciences, University of Lethbridge, AB, Canada*

9

10   \*corresponding author. Email addresses: [symon.mezbahuddin@gov.ab.ca](mailto:symon.mezbahuddin@gov.ab.ca),

11   [mezbahud@ualberta.ca](mailto:mezbahud@ualberta.ca).

12    **Abstract**

13            Water table depth (WTD) effects on net ecosystem CO<sub>2</sub> exchange of boreal peatlands are  
14   largely mediated by hydrological effects on peat biogeochemistry, and eco-physiology of  
15   peatland vegetation. Lack of representation of these effects in carbon models currently limits our  
16   predictive capacity for changes in boreal peatland carbon deposits under potential future drier  
17   and warmer climates. We examined whether a process-level coupling of a prognostic WTD with  
18   1) oxygen transport which controls energy yields from microbial and root oxidation-reduction  
19   reactions, and 2) vascular and non-vascular plant water relations could explain mechanisms that  
20   control variations in net CO<sub>2</sub> exchange of a boreal fen under contrasting WTD conditions i.e.  
21   shallow vs. deep WTD. This coupling of eco-hydrology and biogeochemistry algorithms in a  
22   process-based ecosystem model *ecosys* was tested against net ecosystem CO<sub>2</sub> exchange  
23   measurements in a Western Canadian boreal fen peatland over a period of drier weather driven  
24   gradual WTD drawdown. A May-October WTD drawdown of ~0.25 m from 2004 to 2009  
25   hastened oxygen transport to microbial and root surfaces, enabling greater microbial and root  
26   energy yields, and peat and litter decomposition, which raised modelled ecosystem respiration  
27   ( $R_e$ ) by 0.26  $\mu\text{mol CO}_2 \text{ m}^{-2} \text{ s}^{-1}$  per 0.1 m of WTD drawdown. It also augmented nutrient  
28   mineralization, and hence root nutrient availability and uptake, which resulted in improved leaf  
29   nutrient (nitrogen) status that facilitated carboxylation, and raised modelled vascular gross  
30   primary productivity (GPP) and plant growth. The increase in modelled vascular GPP exceeded  
31   declines in modelled non-vascular (moss) GPP due to greater shading from increased vascular  
32   plant growth, and moss drying from near surface peat desiccation, thereby causing a net increase  
33   in modelled growing season GPP by 0.39  $\mu\text{mol CO}_2 \text{ m}^{-2} \text{ s}^{-1}$  per 0.1 m of WTD drawdown.  
34   Similar increases in GPP and  $R_e$  left no significant WTD effects on modelled seasonal and

35 interannual variations in net ecosystem productivity (NEP). These modelled trends were  
36 corroborated well by eddy covariance measured hourly net CO<sub>2</sub> fluxes (modelled vs. measured:  
37  $R^2\sim0.8$ , slopes $\sim1\pm0.1$ , intercepts $\sim0.05\text{ }\mu\text{mol m}^{-2}\text{ s}^{-1}$ ), hourly measured automated chamber net  
38 CO<sub>2</sub> fluxes (modelled vs. measured:  $R^2\sim0.7$ , slopes $\sim1\pm0.1$ , intercepts $\sim0.4\text{ }\mu\text{mol m}^{-2}\text{ s}^{-1}$ ), and  
39 other biometric and laboratory measurements. Modelled drainage as an analog for WTD  
40 drawdown induced by climate change driven drying showed that this boreal peatland would  
41 switch from a large carbon sink (NEP $\sim160\text{ g C m}^{-2}\text{ yr}^{-1}$ ) to carbon neutrality (NEP $\sim10\text{ g C m}^{-2}$   
42 yr $^{-1}$ ) should water table deepen by a further  $\sim0.5$  m. This decline in projected NEP indicated that  
43 a further WTD drawdown at this fen would eventually lead to a decline in GPP due to water  
44 limitation. Therefore, representing the effects of interactions among hydrology, biogeochemistry  
45 and plant physiological ecology on ecosystem carbon, water, and nutrient cycling in global  
46 carbon models would improve our predictive capacity for changes in boreal peatland carbon  
47 sequestration under changing climates.

48 **1. Introduction**

49 Northern boreal peatlands have been accumulating carbon (C) at a rate of about 20-30 g  
50  $\text{m}^{-2} \text{ yr}^{-1}$  over several thousand years (Gorham, 1991; Turunen et al., 2002). Drier and warmer  
51 future climates can affect the resilience of long-term boreal peatland C stocks by lowering water  
52 table (WT) that can halt or even reverse the C accumulation in boreal peatlands (Limpens et al.,  
53 2008; Dise, 2009; Frolking et al., 2011). To maintain and protect the C sequestration potentials  
54 of boreal peatlands we need an improved predictive capacity of how these C stocks would  
55 behave under future drier and warmer climates. However, boreal peatland C processes are  
56 currently under-represented in global C models largely due to inadequate simulation of  
57 hydrologic feedbacks to C cycles (St-Hilaire et al., 2010; Sulman et al., 2012). This can be  
58 overcome by integrating interactions between eco-hydrology of peatland vegetation, and peat  
59 biogeochemistry into finer resolution process models that can eventually be scaled up into larger  
60 spatial and temporal scale C models (Waddington et al., 2015).

61 The hydrologic feedbacks to boreal peatland C processes are largely mediated by water  
62 table depth (WTD) variation and its effects on peat-microbe-plant-atmosphere exchanges of C,  
63 energy, water and nutrients (Grant et al., 2012). WTD drawdown can affect net ecosystem  
64 productivity (NEP) of boreal peatlands through its effects on ecosystem respiration ( $R_e$ ) and  
65 gross primary productivity (GPP). Receding WT can cause peat pore drainage that enhances  
66 microbial O<sub>2</sub> availability, energy yields, growth and decomposition and hence increases  $R_e$   
67 (Sulman et al., 2009, 2010; Cai et al., 2010; Flanagan and Syed, 2011; Peichl et al., 2014). The  
68 rate of increase in  $R_e$  due to the WTD drawdown may vary with peat moisture retention and  
69 quality of peat forming substrates (Preston et al., 2012). For instance, peats with low moisture  
70 retention exhibit more rapid pore drainage than those with high moisture retention thus causing

71 more increase in  $R_e$  for similar WTD drawdowns (Parmentier et al., 2009; Sulman et al., 2009,  
72 2010; Cai et al., 2010). Peats formed from *Sphagnum* mosses degrade at rates slower than those  
73 formed from remains of vascular plants (Moore and Basiliko, 2006). So for similar WTD  
74 drawdowns, moss peats would generate less increase in microbial decomposition and hence  $R_e$   
75 than would sedge, reed or woody peats (Updegraff et al., 1995). Continued WTD drawdown can  
76 also cause near surface peat desiccation from inadequate recharge through capillary rise from  
77 deeper WT. Desiccation of near surface or shallow peat layers can cause a reduction in microbial  
78 decomposition that can partially or fully offset the increased decomposition in the deeper peat  
79 layers thereby yielding indistinct net effects of WTD drawdown on  $R_e$  (Dimitrov et al., 2010a).

80 The interactions between WTD and GPP vary across peatlands depending upon peat  
81 forming vegetation. For instance, increased aeration due to WTD drawdown enhances root O<sub>2</sub>  
82 availability and growth in vascular plants (Lieffers and Rothwell, 1987; Murphy et al., 2009).  
83 Enhanced root growth is also associated with greater root nutrient availability and uptake from  
84 more rapid mineralization facilitated by greater microbial energy yields, growth and  
85 decomposition under deeper WT (Choi et al., 2007). Greater root nutrient uptake in turns  
86 increases the rate of vascular CO<sub>2</sub> fixation and hence GPP (Sulman et al., 2009, 2010; Cai et al.,  
87 2010; Flanagan and Syed, 2011; Peichl et al., 2014). WTD drawdown, however, does not affect  
88 the non-vascular (e.g., moss) GPP in the same way it does the vascular GPP (Lafleur et al.,  
89 2005). Non-vascular plants mostly depend upon the water available for uptake in the near surface  
90 or shallow peat layers (Dimitrov et al., 2011). These layers can drain quickly with receding WT  
91 and thus have to depend on moisture supply through capillary rise from deeper WT (Dimitrov et  
92 al., 2011; Peichl et al., 2014). If recharge through the capillary rise is not adequate, near surface  
93 peat desiccation occurs which slows moss water uptake, causes eventual drying of mosses and

94 reduces moss GPP (Lafleur et al., 2005; Riutta 2008; Sonnentag et al., 2010; Sulman et al., 2010;  
95 Dimitrov et al., 2011; Kuiper et al., 2014; Peichl et al., 2014). Near surface peat desiccation also  
96 suppresses vascular root water uptake from the desiccated layers (Lafleur et al., 2005; Dimitrov  
97 et al., 2011). But enhanced root growth and elongation facilitated by improved O<sub>2</sub> status in the  
98 newly aerated deeper peat layers under deeper WT enables vascular roots to take up water from  
99 wetter deeper layers (Dimitrov et al., 2011). If deeper root water uptake offsets the reduction in  
100 water uptake from desiccated near surface layers, vascular transpiration ( $T$ ), canopy stomatal  
101 conductance ( $g_c$ ) and hence GPP are sustained under deeper WT (Dimitrov et al., 2011). But if  
102 the WT falls below certain threshold level under which deeper root water uptake can no longer  
103 sustain vascular  $T$ ,  $g_c$  and hence vascular GPP declines (Lafleur et al., 2005; Wu et al., 2010).

104 WTD variation can thus affect boreal peatland NEP through its effects on peat moisture  
105 and aeration and consequent root and microbial oxidation-reduction reactions and energy yields.  
106 To predict how boreal peatlands would behave under future drier and warmer climates, a  
107 peatland C model thus needs to simulate WTD dynamics that determine the boundary between  
108 aerobic and anaerobic zones and controls peat biogeochemistry. However, most of the current  
109 process-based peatland C models either do not simulate a continuous anaerobic zone below a  
110 prognostic WT (e.g., Baker et al., 2008; Schaefer et al., 2008; Tian et al., 2010), or do not  
111 simulate peat saturation since any water in excess of field capacity is drained in those models  
112 (e.g., Gerten et al., 2004; Krinner et al., 2005; Weng and Luo, 2008). Moreover, instead of  
113 explicitly simulating the above-described hydrological and biological interactions between peat  
114 aeration and biogeochemistry, most of those models use scalar functions of soil moisture  
115 contents to inhibit  $R_e$  and GPP under low or high moisture conditions (e.g., Frolking et al., 2002;  
116 Zhang et al., 2002; Bond-Lamberty et al., 2007; St-Hilaire et al., 2010; Sulman et al., 2012).

117 Consequently, those peatland C models could not simulate declines in GPP and  $R_e$  due to  
118 shallow WT while simulating WTD effects on CO<sub>2</sub> exchange of peatlands across northern US  
119 and Canada (Sulman et al., 2012). Furthermore, the approach of using scalar functions to  
120 simulate moisture limitations to GPP and  $R_e$  requires site-specific parameterization of model  
121 algorithms which reduces scalability of those peatland C models.

122 **1.1. Objective and rationale**

123 In this study, we tested a process-based ecosystem model *ecosys* against eddy covariance  
124 (EC) net CO<sub>2</sub> fluxes measured over a drying period from 2004 to 2009 in a western Canadian  
125 boreal fen peatland in Alberta, Canada (will be termed as WPL hereafter) (Syed et al., 2006;  
126 Flanagan and Syed, 2011). The objective was to test whether the coupling of a dynamic WTD  
127 that arises from vertical and lateral water fluxes as a function of a soil moisture retention scheme  
128 with 1) oxygen transport, 2) microbial and root oxidation-reduction reactions and energy yields,  
129 and 3) root, microbial and plant growth and uptake within a soil-plant-microbe-atmosphere  
130 water, C and nutrient (nitrogen, phosphorus) scheme in an ecosystem process model could  
131 explain underlying processes that govern hydrological effects on net CO<sub>2</sub> exchange of a northern  
132 boreal fen under contrasting WTD conditions (e.g., shallower vs. deeper WTD). This study  
133 would reconcile our knowledge on the feedback mechanisms among hydrology, eco-physiology,  
134 and biogeochemistry of peatlands which are predominantly based upon inferences drawn from  
135 EC-gap filled values that include empirically modelled estimates. It would also provide us with a  
136 better insight into- and an improved predictive capacity of- how carbon deposits in northern  
137 boreal peatlands would behave under changing climates. Rigorous site-scale testing of coupled  
138 eco-hydrology and biogeochemistry algorithms in ecosystem process models such as *ecosys*

139 would also provide us with important insights on how to improve large-scale representation of  
140 these processes into next generation land surface models.

141 **1.2. Hypotheses**

142 In an eddy covariance (EC) study, Flanagan and Syed (2011) found no net effect of a  
143 weather driven WTD drawdown on NEP of WPL over 2004-2009. From the regressions of EC-  
144 derived GPP and  $R_e$  on site measured WTD, they inferred that the absence of a net WTD effect  
145 on NEP was caused by similar increases in GPP and  $R_e$  with WTD drawdown. We hypothesized  
146 that coupled eco-hydrology and biogeochemistry algorithms in *ecosys* would be able to simulate  
147 and explain underlying mechanisms of these effects of WTD drawdown on GPP and  $R_e$  and  
148 hence NEP at the WPL. We tested the following four central hypotheses:

149 (1) WTD drawdown would increase  $R_e$  of the northern fen at the WPL. This effect of WTD  
150 drawdown on  $R_e$  would be modelled by simulation of peat pore drainage and improved peat  
151 aeration that would increase the energy yields from aerobic microbial decomposition and hence  
152 would increase  $R_e$ .

153 (2) WTD drawdown would increase GPP of the northern fen at the WPL. This effect of WTD  
154 drawdown on GPP would be modelled by simulating enhanced microbial activity due to WTD  
155 drawdown that would cause more rapid nutrient mineralization and greater root nutrient  
156 availability and uptake, greater leaf nutrient concentrations and hence increased GPP.

157 (3) Increase in  $R_e$  with WTD drawdown (hypothesis 1) would cease should WTD fall below a  
158 threshold depth. This threshold WTD effect on  $R_e$  would be modelled by simulating inadequate  
159 recharge of the near surface peat layers through capillary rise from the deeper WTD below the  
160 threshold level that would cause desiccation of those layers. Drying of near surface peat layers

161 and the surface residue would reduce near surface and surface peat respiration that would  
162 partially offset the increase in deeper peat respiration due to aeration.

163 (4) Net effect of threshold WTD on GPP would be driven by the balance between how WTD  
164 would affect vascular vs. non-vascular GPP. This threshold WTD effect on GPP would be  
165 modelled by simulating vascular vs. non-vascular water relations under deeper WTD below the  
166 threshold level. Near surface peat desiccation in hypothesis 3 would reduce peat water potential  
167 and hydraulic conductivity and hence vascular and non-vascular water uptake from desiccated  
168 near surface layers. Since non-vascular mosses depend mainly on near surface peat layers for  
169 moisture supply, reduction in moss water uptake would cause a reduction in moss water potential  
170 and hence moss GPP. On the contrary, suppression of vascular root water uptake from desiccated  
171 near surface layers under deeper WT would be offset by increased deeper root water uptake from  
172 newly aerated deeper peat layers with higher water potentials that would sustain vascular canopy  
173 water potential ( $\psi_c$ ), canopy stomatal conductance ( $g_c$ ) and GPP.

174 **2. Methods**

175 **2.1. Model development**

176 *Ecosys* is a process-based ecosystem model which simulated 3D water, energy, carbon  
177 and nutrient (nitrogen, phosphorus) cycles in different peatlands (Dimitrov et al., 2011; Grant et  
178 al., 2012; Sulman et al., 2012; Mezbahuddin et al., 2014, 2015, 2016). *Ecosys* algorithms that  
179 govern the modelled effects of WTD variations on peatland net CO<sub>2</sub> exchange are described  
180 below. These algorithms in *ecosys* are derived from published independent basic research which  
181 describe eco-hydrological and biogeochemical mechanisms that govern carbon, nutrient (N, P),  
182 water, and energy balance of a typical boreal peatland ecosystem (Fig. 1). *Ecosys* algorithms  
183 which are related to our hypotheses are depicted as a flowchart (Fig. 1) and cited as equations

184 within the text. These equations are also listed in sections S1-S4 of the supplementary material  
185 with references to their sources for further clarification. These site-independent basic ecosystem  
186 process algorithms in *ecosys* are thus not parameterized for each peatland site. Instead the  
187 coupled algorithms are fed with peatland-specific measurable soil, weather, vegetation and  
188 management inputs to simulate C, nutrient (N, P), water and energy balance of a particular  
189 peatland ecosystem.

190 **2.1.1. Water table depth (WTD)**

191 The WTD in *ecosys* is calculated at the end of each time step as the depth to the top of the  
192 saturated zone below which air-filled porosity is zero (Eq. D32). It is the depth at which lateral  
193 water flux is in equilibrium with the difference between vertical influxes (precipitation) and  
194 effluxes (evapotranspiration). Lateral water transfer between modelled grid cells in *ecosys* and  
195 the adjacent ecosystem occurs to and from a set external WTD (WTD<sub>x</sub>) over a set distance ( $L_t$ )  
196 (Fig. 2). The WTD<sub>x</sub> represents average watershed WTD with reference to average hummock  
197 surface. The WTD in *ecosys* is thus not prescribed, but rather controls, and is controlled by  
198 lateral and vertical surface and subsurface water fluxes (Eqs. D1-D31). More detail about how  
199 peatland WTD, vertical and lateral soil water flow, and soil moisture retention are modelled in  
200 *ecosys* can be found in Dimitrov et al. (2010b) and Mezbahuddin et al. (2015, 2016).

201 **2.1.2. Heterotrophic respiration and WTD**

202 WTD fluctuation in *ecosys* determines the boundary between and the extent of aerobic vs.  
203 anaerobic soil zones. So WTD fluctuation affects *ecosys*'s algorithms of organic oxidation-  
204 reduction transformations and microbial energy yields, which drive microbial growth, substrate  
205 decomposition and uptake (Fig. 1) (Eqs. A1-A30). Organic transformations in *ecosys* occur in a  
206 residue layer and in each of the user defined soil layers within five organic matter-microbe

207 complexes i.e., coarse woody litter, fine non-woody litter, animal manure, particulate organic C  
208 and humus (Fig. 1). Each of the complexes has three decomposition substrates i.e., solid organic  
209 C, sorbed organic C and microbial residue C; the decomposition agent i.e., microbial biomass;  
210 and the decomposition product i.e., dissolved organic C (DOC) (Fig. 1). Rates of the  
211 decomposition and resulting DOC production in each of the complexes is a first-order function  
212 of the fraction of substrate colonized by active biomasses ( $M$ ) of diverse microbial functional  
213 types (MFTs). The MFTs in *ecosys* are obligate aerobes (bacteria and fungi), facultative  
214 anaerobes (denitrifiers), obligate anaerobes (fermenters), heterotrophic (acetotrophic) and  
215 autotrophic (hydrogenotrophic) methanogens, and aerobic and anaerobic heterotrophic  
216 diazotrophs (non-symbiotic N<sub>2</sub> fixers) (Fig. 1) (Eqs. A1-A2, A4). Biomass ( $M$ ) growth of each of  
217 the MFTs (Eq. A25a) is calculated from its DOC uptake (Fig. 1) (Eq. A21). The rate of  $M$   
218 growth is driven by energy yield from growth respiration ( $R_g$ ) (Eq. A20) that is calculated by  
219 subtracting maintenance respiration ( $R_m$ ) (Eq. A18) from heterotrophic respiration ( $R_h$ ) (Eq.  
220 A11). The values of  $R_h$  are driven by oxidation of DOC (Eq. A13). DOC oxidation may be  
221 limited by microbial O<sub>2</sub> reduction (Eq. A14) driven by microbial O<sub>2</sub> demand (Eq. A16) and  
222 constrained by O<sub>2</sub> diffusion calculated from aqueous O<sub>2</sub> concentrations in soil ([O<sub>2s</sub>]) (Eq. A17).  
223 Values of [O<sub>2s</sub>] are maintained by convective-dispersive transport of O<sub>2</sub> from the atmosphere to  
224 gaseous and aqueous phases of the soil surface layer (Eq. D41), by convective-dispersive  
225 transport of O<sub>2</sub> through gaseous and aqueous phases in adjacent soil layers (Eqs. D42, D44), and  
226 by dissolution of O<sub>2</sub> from gaseous to aqueous phases within each soil layer (Eq. D39).

227 Shallow WTD in *ecosys* can cause lower air-filled porosity ( $\theta_g$ ) in the wetter peat layers  
228 above the WT. Lower  $\theta_g$  reduces O<sub>2</sub> diffusivity in the gaseous phase ( $D_g$ ) (Eq. D44) and gaseous  
229 O<sub>2</sub> transport (Eqs. D41-D42) in these layers. Peat layers below the WT have zero  $\theta_g$  that prevents

230 gaseous O<sub>2</sub> transport in these layers. So, under shallow WT, [O<sub>2s</sub>] relies more on O<sub>2</sub> transport  
231 through the slower aqueous phase (Eq. D42) which causes a decline in [O<sub>2s</sub>]. Decline in [O<sub>2s</sub>]  
232 slows O<sub>2</sub> uptake (Eq. A17) and hence  $R_h$  (Eq. A14),  $R_g$  (Eq. A20) and growth of  $M$  (Eq. A25).  
233 Lower  $M$  slows decomposition of organic C (Eqs. A1-A2) and production of DOC which further  
234 slows  $R_h$  (Eq. A13),  $R_g$  and growth of  $M$  (Fig. 1). Although some MFTs can sustain DOC  
235 oxidation by reducing alternative electron acceptors (e.g., methanogens reducing acetate or CO<sub>2</sub>  
236 to CH<sub>4</sub>, and denitrifiers reducing NO<sub>x</sub> to N<sub>2</sub>O or N<sub>2</sub>), lower energy yields from these reactions  
237 reduce  $R_g$  (Eq. A21), and hence  $M$  growth, organic C decomposition and subsequent DOC  
238 production (Fig. 1). Slower decomposition of organic C under low [O<sub>2s</sub>] also causes slower  
239 decomposition of organic nitrogen (N) and phosphorus (P) (Eq. A7) and production of dissolved  
240 organic nitrogen (DON) and phosphorus (DOP), which causes slower uptake of microbial N and  
241 P (Eq. A22) and growth of  $M$  (Eq. A29) (Fig. 1). Slower  $M$  growth causes slower mineralization  
242 (Eq. A26), and hence lowers aqueous concentrations of NH<sub>4</sub><sup>+</sup>, NO<sub>3</sub><sup>-</sup> and H<sub>2</sub>PO<sub>4</sub><sup>-</sup> (Fig. 1).

243 WTD drawdown can increase  $\theta_g$  that results in greater  $D_g$  (Eq. D44) and more rapid  
244 gaseous O<sub>2</sub> transport. A consequent rise in [O<sub>2s</sub>] increases O<sub>2</sub> uptake (Eq. A17) and  $R_h$  (Eq. A14),  
245  $R_g$  (Eq. A20) and growth of  $M$  (Eq. A25). Larger  $M$  hastens decomposition of organic C (Eqs.  
246 A1-A2) and production of DOC which further hastens  $R_h$  (Eq. A13),  $R_g$  and growth of  $M$ . More  
247 rapid decomposition of organic C under adequate [O<sub>2s</sub>] in this period also causes more rapid  
248 decomposition of organic N and P (Eq. A7) and production of DON and DOP, which increases  
249 uptake of microbial N and P (Eq. A22) and growth of  $M$  (Eq. A29) (Fig. 1). Rapid  $M$  growth  
250 causes rapid mineralization (Eq. A26), and hence greater aqueous concentrations of NH<sub>4</sub><sup>+</sup>, NO<sub>3</sub><sup>-</sup>  
251 and H<sub>2</sub>PO<sub>4</sub><sup>-</sup> (Fig. 1).

252 When WTD recedes below a certain threshold level, capillary rise from the WT can no  
253 longer support adequate recharge of the near surface peat layers and the surface litter (Eqs. D9,  
254 D12). It causes desiccation of the residue and the near surface peat layers thereby causing a  
255 reduction in water potential ( $\psi_s$ ) and an increase in aqueous microbial concentrations ( $[M]$ ) in  
256 each of these layers (Eq. A15). Increased  $[M]$  caused by the peat desiccation reduces microbial  
257 access to the substrate for decomposition in each of the desiccated layers and reduces  $R_h$  (Eq.  
258 A13). Reduction in  $R_h$  is calculated in *ecosys* from competitive inhibition of microbial exo-  
259 enzymes with increasing concentrations (Eq. A4) (Lizama and Suzuki, 1991).

260 **2.1.3. WTD effects on vascular gross primary productivity**

261 *Ecosys* simulates effects of WTD variation on vascular GPP from WTD variation effects  
262 on root O<sub>2</sub> and nutrient availability and root growth and uptake. Root O<sub>2</sub> and nutrient uptake in  
263 *ecosys* are coupled with a hydraulically driven soil-plant-atmosphere water scheme. Root growth  
264 in each vascular plant population in *ecosys* is calculated from its assimilation of the non-  
265 structural C product of CO<sub>2</sub> fixation ( $\sigma_C$ ) (Eq. C20). Assimilation is driven by  $R_g$  (Eq. C17)  
266 remaining after subtracting  $R_m$  (Eq. C16) from autotrophic respiration ( $R_a$ ) (Eq. C13) driven by  
267 oxidation of  $\sigma_C$  (Eq. C14). Oxidation in roots may be limited by root O<sub>2</sub> reduction (Eq. C14b)  
268 which is driven by root O<sub>2</sub> demand to sustain C oxidation and nutrient uptake (Eq. C14e), and  
269 constrained by O<sub>2</sub> uptake controlled by concentrations of aqueous O<sub>2</sub> in the soil ( $[O_{2s}]$ ) and roots  
270 ( $[O_{2r}]$ ) (Eq. C14d). Values of  $[O_{2s}]$  and  $[O_{2r}]$  are maintained by convective-dispersive transport  
271 of O<sub>2</sub> through soil gaseous and aqueous phases and root gaseous phase (aerenchyma)  
272 respectively and by dissolution of O<sub>2</sub> from soil and root gaseous to aqueous phases (Eqs. D39-  
273 D45). O<sub>2</sub> transport through root aerenchyma depends on species-specific values used for root air-  
274 filled porosity ( $\theta_{pr}$ ) (Eq. D45). Shallow WTD and resultant high peat moisture content in *ecosys*

275 can cause low  $\theta_g$  that reduces soil O<sub>2</sub> transport, forcing root O<sub>2</sub> uptake to rely more on [O<sub>2r</sub>] and  
276 hence on root O<sub>2</sub> transport determined by  $\theta_{pr}$ . If this transport is inadequate, decline in [O<sub>2r</sub>]  
277 slows root O<sub>2</sub> uptake (Eqs. C14c-d) and hence  $R_a$  (Eq. C14b),  $R_g$  (Eq. C17) and root growth (Eq.  
278 C20b) and root N and P uptake (Eqs. C23b, d, f) (Fig. 1). Root N and P uptake under shallow  
279 WT is further slowed by reductions in aqueous concentrations of NH<sub>4</sub><sup>+</sup>, NO<sub>3</sub><sup>-</sup> and H<sub>2</sub>PO<sub>4</sub><sup>-</sup> (Eqs.  
280 C23a, c, e) from slower mineralization of organic N and P (Fig. 1). Slower root N and P uptake  
281 reduces concentrations of non-structural N and P products of root uptake ( $\sigma_N$  and  $\sigma_P$ ) with  
282 respect to that of  $\sigma_C$  in leaves (Eq. C11), thereby slowing CO<sub>2</sub> fixation (Eq. C6) and GPP.

283 WTD drawdown facilitates rapid  $D_g$  which allows root O<sub>2</sub> demand to be almost entirely  
284 met from [O<sub>2s</sub>] (Eqs. C14c-d) and so enables more rapid root growth and N and P uptake (Eqs.  
285 C23b, d, f). Increased root growth and nutrient uptake is further stimulated by increased aqueous  
286 concentrations of NH<sub>4</sub><sup>+</sup>, NO<sub>3</sub><sup>-</sup> and H<sub>2</sub>PO<sub>4</sub><sup>-</sup> (Eqs. C23a, c, e) from more rapid mineralization of  
287 organic N and P during deeper WT (Fig. 1). Greater root N and P uptake increases  
288 concentrations of  $\sigma_N$  and  $\sigma_P$  with respect to  $\sigma_C$  in leaves (Eq. C11), thereby facilitating rapid CO<sub>2</sub>  
289 fixation (Eq. C6) and GPP. When WT falls below a certain threshold, inadequate capillary rise  
290 (Eqs. A9, A12) from deeper WT causes near-surface peat desiccation that reduces soil water  
291 potential ( $\psi_s$ ) and raises soil hydraulic resistance ( $\Omega_s$ ) (Eq. B9), thereby forcing lower root water  
292 uptake ( $U_w$ ) from desiccated layers (Fig. 1) (Eq. B6). However, deeper rooting facilitated by  
293 increased [O<sub>2s</sub>] under deeper WT can sustain  $U_w$  (Eq. B6) from wetter deeper peat layers with  
294 higher  $\psi_s$  and lower  $\Omega_s$  (Eq. B9). If  $U_w$  from the deeper wetter layers cannot offset the  
295 suppression in  $U_w$  from desiccated near surface layers, the resultant net decrease in  $U_w$  causes a  
296 reduction in root, canopy and turgor potentials ( $\psi_r$ ,  $\psi_c$  and  $\psi_t$ ) (Eq. B4) and hence  $g_c$  (Eq. B2b) in

297 *ecosys* when equilibrating  $U_w$  with transpiration ( $T$ ) (Eq. B14). Lower  $g_c$  reduces CO<sub>2</sub> diffusion  
298 into the leaves thereby reducing CO<sub>2</sub> fixation (Eq. C6) and GPP (Eq. C1) (Fig. 1).

299 **2.1.4. WTD effects on non-vascular gross primary productivity**

300 *Ecosys* simulates non-vascular plants (e.g., mosses) as tiny plants with no stomatal  
301 regulations that grow on modelled hummock and hollow grid cells (Dimitrov et al., 2011).  
302 Model input for moss population is usually larger and hence intra-specific competition for lights  
303 and nutrients is greater so that individual moss plant and moss belowground growth (i.e. root like  
304 structures for water and nutrient uptake) are smaller (Eq. C21b). Shallower belowground growth  
305 of simulated mosses in *ecosys* means the water uptake of mosses are mostly confined to the near  
306 surface peat layers. When WT deepens past a threshold level, inadequate capillary rise (Eqs. D9,  
307 D12) causes near-surface peat desiccation, thereby reducing  $\psi_s$  and increasing  $\Omega_s$  (Eq. B9) of  
308 those layers (Fig. 1). It causes a reduction in moss canopy water potential ( $\psi_c$ ) while  
309 equilibrating moss evaporation with moss  $U_w$  (Eq. B6). Reduced moss  $\psi_c$  causes a reduction in  
310 moss carboxylation rate (Eqs. C3, C6a) and moss GPP (Fig. 1) (Eq. C1).

311 **2.2. Modelling experiment**

312 **2.2.1. Study site**

313 The peatland eco-hydrology and biogeochemistry algorithms in *ecosys* were tested in this  
314 study against measurements of WTD and ecosystem net CO<sub>2</sub> fluxes at a flux station of the  
315 Fluxnet-Canada Research Network established at the WPL (latitude: 54.95°N, longitude:  
316 112.47°W). The study site is a moderately nutrient-rich treed fen peatland within the Central  
317 Mixed-wood Sub-region of Boreal Alberta, Canada. Peat depth around the flux station was about  
318 2 m. This peatland is dominated by stunted trees of black spruce (*Picea mariana*) and tamarack  
319 (*Larix laricina*) with an average canopy height of 3 m. High abundance of a shrub species *Betula*

320 *pumila* (dwarf birch), and the presence of a wide range of mosses e.g., *Sphagnum* spp., feather  
321 moss, and brown moss characterize the under-storey vegetation of WPL. The topographic,  
322 climatic, edaphic and vegetative characteristics of this site were described in more details by  
323 Syed et al. (2006).

324 **2.2.2. Field data sets**

325 *Ecosys* model inputs of half hourly weather variables i.e. incoming shortwave and  
326 longwave radiation, air temperature ( $T_a$ ), wind speed, precipitation and relative humidity during  
327 2003-2009 were measured by Syed et al. (2006) and Flanagan and Syed (2011) at the  
328 micrometeorological station installed at the WPL. To test the adequacy of WTD simulation in  
329 *ecosys*, modelled outputs of hourly WTD were tested against WTD measured at the WPL with  
330 respect to average hummock surface by Flanagan and Syed (2011). To examine how well *ecosys*  
331 simulated net ecosystem CO<sub>2</sub> exchange at the WPL, we tested hourly modelled net ecosystem  
332 CO<sub>2</sub> fluxes against hourly averaged measurements (average of two half-hourly) collected by  
333 Syed et al. (2006) and Flanagan and Syed (2011) by using eddy covariance (EC) micro-  
334 meteorological approach. Each of these EC-measured net CO<sub>2</sub> fluxes consisted of an eddy flux  
335 and a storage flux (Syed et al. 2006). Erroneous flux measurements due to stable air conditions  
336 were screened out with the use of a minimum friction velocity ( $u^*$ ) threshold of 0.15 m s<sup>-1</sup> (Syed  
337 et al. 2006). The net CO<sub>2</sub> fluxes that survived the quality control were used to derive half hourly  
338  $R_e$  (=nighttime net CO<sub>2</sub> fluxes) and GPP (=daytime net CO<sub>2</sub> fluxes –  $R_e$ ) (Barr et al., 2004; Syed  
339 et al., 2006). To derive daily, seasonal and annual estimates of GPP, and  $R_e$ , the data gaps  
340 resulting from the quality control were filled based on empirical relationships between soil  
341 temperature at a shallow depth (0.05 m) and measured half hourly  $R_e$ , and between incoming  
342 shortwave radiation and measured half hourly GPP using 15-days moving windows. The gap-

343 filled  $R_e$  and GPP were then summed up for each half hour to fill NEP data gaps to derive daily,  
344 seasonal and annual estimates of EC-gap filled NEP (Barr et al., 2004; Syed et al., 2006).

345 Soil CO<sub>2</sub> fluxes measured by automated chambers can provide a valuable supplement to  
346 EC CO<sub>2</sub> fluxes in testing modelled respiration by providing more continuous measurements than  
347 EC. So, we tested our modelled outputs against half-hourly automated chamber measurements by  
348 Cai et al. (2010) at the WPL. These CO<sub>2</sub> flux measurements were carried out during ice-free  
349 periods (May-October) of 2005 and 2006 over both hummocks and hollows by using a total of 9  
350 non-steady state automatic transparent chambers (Cai et al., 2010). Along with soil respiration  
351 these chamber CO<sub>2</sub> fluxes included fixation and autotrophic respiration from dwarf shrubs, herbs  
352 and mosses (Cai et al., 2010).

353 Modelled WTD effects on peatland biogeochemistry and hence on peatland nutrient and  
354 carbon cycling were also corroborated against leaf nitrogen concentrations, foliar N to P ratios, N  
355 mineralization, and rooting depths biometrically measured at either our site or at sites that had  
356 similar peat substrates, hydrology and/or plant functional types. Needles of black spruce and  
357 tamarack, and leaves of dwarf birch were sampled over our study site during mid-summer of  
358 2004 for foliar nutrient content analyses (Syed et al., 2006). Leaf nitrogen contents were  
359 analyzed on N<sub>2</sub> gas that were generated from reduction of dried leaf tissues in an elemental  
360 analyzer and quantified using a gas isotope ratio mass spectrometer (Syed et al., 2006). Leaf  
361 phosphorus contents were analyzed on black spruce and tamrack needle leaf tissues that were  
362 dry-ashed and then digested using a dilute HNO<sub>3</sub> and HCl mixture and then quantified using an  
363 Inductively Coupled Plasma (ICP) spectroscopic analysis technique (Syed et al., 2006).

364      **2.2.3. Model run**

365            *Ecosys* model run to simulate WTD effects on net CO<sub>2</sub> exchange of WPL had a  
366            hummock and a hollow grid cell that exchanged water, heat, carbon and nutrients (N, P) between  
367            them and with surrounding vertical and lateral boundaries (Fig. 2). The hollow grid cell had near  
368            surface peat layer that was 0.3 m thinner than the hummock cell representing a hummock-hollow  
369            surface difference of 0.3 m observed in the field (Long, 2008) (Fig. 2). Any depth with respect to  
370            the modelled hollow surface would thus be 0.3 m shallower than the depth with respect to the  
371            modelled hummock surface.

372            Peat organic and chemical properties at different depths of the WPL were represented in  
373            *ecosys* by inputs from measurements either at the site (e.g., Syed et al., 2006; Flanagan and Syed,  
374            2011) or at similar nearby sites (e.g., Rippy and Nelson, 2007) (Fig. 2). *Ecosys* was run for a spin  
375            up period of 1961-2002 under repeating 7-year sequences of hourly weather data (shortwave and  
376            longwave radiation, air temperature, wind speed, humidity and precipitation) recorded at the site  
377            from 2003 to 2009. There was a drying trend observed from 2003 to 2009 due to diminishing  
378            precipitation that caused WTD drawdown in the watershed in which WPL is located, which  
379            lowered the WT of this fen peatland (Flanagan and Syed, 2011). To accommodate the gradual  
380            drying effects of catchment hydrology on modelled fen peatland WTD, we set the WTD<sub>x</sub> at  
381            different levels based on the annual wetness of weather, e.g., shallow, intermediate, and deep  
382            (WTD<sub>x</sub>=0.19, 0.35 and 0.72 m below the hummock surface, or 0.11 m above and 0.05 and 0.42  
383            m below the hollow surface) (Fig. 2). There was no exchange of water through lower model  
384            boundary to represent the presence of nearly impermeable clay sediment underlying the peat  
385            (Syed et al., 2006) (Fig. 2). Variations in peat surface with WTD variations, which is an

386 important hydrologic self-regulation of boreal peatlands (Dise, 2009), was not represented in this  
387 version of *ecosys*.

388 At the start of the spin up run, the hummock grid cell was seeded with an evergreen  
389 needle leaf and a deciduous needle leaf over-storey plant functional types (PFT) to represent the  
390 black spruce and tamarack trees at the WPL. The hollow grid cell was seeded with only the  
391 deciduous needle leaf over-storey PFTs since the black spruce trees at the WPL only grew on the  
392 raised areas. Each of the modelled hummock and the hollow was also seeded with a deciduous  
393 broadleaved vascular (to represent dwarf birch) and a non-vascular (to represent mosses) under-  
394 storey PFTs. The planting densities were such that the population densities of the black spruce,  
395 tamarack, dwarf birch and moss PFTs were 0.16, 0.14, 0.3, and 500 m<sup>-2</sup> respectively at the end of  
396 the spin up run so as to best represent field vegetation (Syed et al., 2006; Mezbahuddin et al.,  
397 2016). To include wetland adaptation, we used a root porosity ( $\theta_{pr}$ ) value of 0.1 for the two over-  
398 storey PFTs and a higher  $\theta_{pr}$  value of 0.3 for the under-storey vascular PFT to represent better  
399 wetland adaptation in the under-storey than the over-storey PFTs. These  $\theta_{pr}$  values were used in  
400 calculating root O<sub>2</sub> transport through aerenchyma (Eq. D45) and did not change with  
401 waterlogging throughout the model run. These  $\theta_{pr}$  values were representatives of root porosities  
402 measured for various northern boreal peatland plant species (Cronk and Fennessy, 2001). Non-  
403 symbiotic N<sub>2</sub> fixation through association of cyanobacteria and mosses are also reported for  
404 Canadian boreal forests (Markham, 2009). This was represented in *ecosys* as N<sub>2</sub> fixation by non-  
405 symbiotic heterotrophic diazotrophs (Eq. A27) in the moss canopy. Further details about *ecosys*  
406 model set up to represent the hydrological, physical and ecological characteristics of WPL can be  
407 found in Mezbahuddin et al. (2016).

408 When the modelled ecosystem attained stable values of net ecosystem CO<sub>2</sub> exchange at  
409 the end of the spin-up run, we continued the spin up run into a simulation run from 2003 to 2009  
410 by using a real-time weather sequence. We tested our outputs from 2004-2009 of the simulation  
411 run against the available site measurements of WTD, net EC CO<sub>2</sub> fluxes and net chamber CO<sub>2</sub>  
412 fluxes over those years.

413 **2.2.4. Model validation**

414 To examine the adequacy of modelling WTD effects on canopy, root and soil CO<sub>2</sub> fluxes  
415 which were summed for net ecosystem CO<sub>2</sub> exchange at the WPL, we spatially averaged hourly  
416 net CO<sub>2</sub> fluxes modelled over the hummock and the hollow to represent a 50:50 hummock-  
417 hollow ratio and then regressed against hourly EC measured net ecosystem CO<sub>2</sub> fluxes for each  
418 year from 2004-2009 with varying WTD. Each of these hourly EC measured net ecosystem CO<sub>2</sub>  
419 fluxes used in these regressions is an average of two half-hourly net CO<sub>2</sub> fluxes measured at a  
420 friction velocity ( $u^*$ ) greater than 0.15 m s<sup>-1</sup> that survived quality control procedure (Sec. 2.2.2).  
421 Model performance was evaluated from regression intercepts ( $a \rightarrow 0$ ), slopes ( $b \rightarrow 1$ ), coefficients  
422 of determination ( $R^2 \rightarrow 1$ ), and root means squares for errors (RMSE  $\rightarrow 0$ ) for each study year to  
423 test whether there was any systematic divergence between the modelled and EC measured CO<sub>2</sub>  
424 fluxes.

425 Similar regressions were performed between modelled and automated chamber measured  
426 net CO<sub>2</sub> fluxes for ice free periods (May-October) of 2005 and 2006 to further test the robustness  
427 of modelled soil respiration under contrasting WTD conditions. Each of the half-hourly  
428 measured chamber net CO<sub>2</sub> fluxes included soil respiration, and fixation and autotrophic  
429 respiration from understorey vegetation (e.g., shrubs, herbs and mosses). So, we combined  
430 modelled soil respiration with modelled fixation and autotrophic respiration from understorey

431 PFTs for comparison against these chamber measured net CO<sub>2</sub> fluxes. We also averaged net CO<sub>2</sub>  
432 flux measurements from all of the 9 chambers for each half hour to accommodate the variations  
433 in those fluxes due to microtopography (e.g., hummock vs. hollow). Two half hourly averaged  
434 values of net CO<sub>2</sub> fluxes were then averaged again to get hourly mean net chamber CO<sub>2</sub> fluxes  
435 for comparison against modelled hourly sums of soil and understorey fluxes averaged over  
436 modelled hummock and hollow. Model performance was evaluated from regression intercepts  
437 ( $a \rightarrow 0$ ), slopes ( $b \rightarrow 1$ ), coefficients of determination ( $R^2 \rightarrow 1$ ), and root means squares for errors  
438 (RMSE  $\rightarrow 0$ ) for each of 2005 and 2006.

439 **2.2.5. Sensitivity of modelled peatland CO<sub>2</sub> exchange to artificial drainage**

440 Large areas of northern boreal peatlands in Canada have been drained primarily for  
441 increased forest and agricultural production since plant productivity in pristine peatlands are  
442 known to be constrained by shallow WTD (Choi et al., 2007). Drainage and resultant WTD  
443 drawdown can affect both GPP and  $R_e$  on a short-term basis and the vegetation composition on a  
444 longer time scale thereby changing overall net CO<sub>2</sub> exchange trajectories of a peatland. To  
445 predict short-term effects of drainage on WTD and hence ecosystem net CO<sub>2</sub> exchange of WPL,  
446 we extended our simulation run into a projection run consisting two 7-yr cycles by using  
447 repeated weather sequences of 2003-2009. While doing so, we forced a stepwise drawdown in  
448 WTD<sub>x</sub> by 1.0 and 2.0 m from that used in spin-up and simulation runs (Fig. 2) in the first  
449 (drainage cycle 1) and the second cycle (drainage cycle 2) respectively. This projection run  
450 would give us a further insight about how the northern boreal peatland of Western Canada would  
451 be affected by further WTD drawdown as a result of drier and warmer weather as well as a  
452 disturbance such as drainage. It would also provide us with a test of how sensitive the modelled

453 C processes were to the changes in model lateral boundary condition as defined by WTD<sub>x</sub> in  
454 *ecosys*.

455 **3. Results**

456 **3.1. Model performance in simulating diurnal variations in ecosystem net CO<sub>2</sub> fluxes**

457 Variations in precipitation can cause change in WTD and consequent variation in diurnal  
458 net CO<sub>2</sub> exchange across years. *Ecosys* simulated hourly EC-measured net CO<sub>2</sub> fluxes well over  
459 2004-2008 with varying precipitation (Table 1a). On a year-to-year basis, regressions of hourly  
460 modelled vs. EC-measured net ecosystem CO<sub>2</sub> fluxes gave intercepts within 0.1  $\mu\text{mol m}^{-2} \text{s}^{-1}$  of  
461 zero, and slopes within 0.1 of one, indicating minimal bias in modelled outputs during each year  
462 from 2004-2008 (Table 1a). On a growing season (May-August) basis, regressions of modelled  
463 on measured hourly net CO<sub>2</sub> fluxes yielded larger positive intercepts from 2004-2009 (Table 1b).

464 The larger intercepts were predominantly caused by modelled overestimation of growing season  
465 day-time CO<sub>2</sub> fluxes. This overestimation was offset by modelled overestimation of night-time  
466 CO<sub>2</sub> fluxes during the winter thus yielding smaller intercepts from throughout-the-year  
467 regressions of modelled vs. EC measured fluxes (Tables 1a vs. b). Values for coefficients of  
468 determination ( $R^2$ ) were  $\sim 0.8$  ( $P < 0.001$ ) for all years from both throughout-the-year and  
469 growing season regressions (Tables 1a, b). RMSEs were  $< 2.0$  and  $\sim 2.5 \mu\text{mol m}^{-2} \text{s}^{-1}$  for whole  
470 year regressions from 2004-2008 (Table 1a) and for growing season regressions from 2004-2009  
471 (Table 1b) respectively. Much of the variations in EC measured CO<sub>2</sub> fluxes that was not  
472 explained by the modelled fluxes could be attributed to a random error of  $\sim 20\%$  in EC  
473 methodology (Wesely and Hart, 1985). This attribution was further corroborated by root mean  
474 squares for random errors (RMSRE) in EC measurements, calculated for forests with similar  
475 CO<sub>2</sub> fluxes from Richardson et al. (2006) that were similar to RMSE (Tables 1a, b). The similar

476 values of RMSE and RMSRE also indicated that further constraint in model testing could not be  
477 achieved without further precision in EC measurements.

478       Regressions of modelled vs. chamber measured net CO<sub>2</sub> fluxes gave  $R^2$  of ~0.7 for ice-  
479 free periods (May-October) of 2005 and 2006 indicated that the variations in soil respiration, and  
480 the fixation and aboveground autotrophic respiration due to WTD drawdown were modelled well  
481 (Table 1c). Smaller intercepts from those regressions meant lower model biases in simulating  
482 soil and understorey CO<sub>2</sub> fluxes under deepening WT (Table 1c). Although the slope was within  
483 0.1 of one in 2005, it was a bit smaller in 2006 indicating lower modelled vs. chamber measured  
484 soil and understorey net CO<sub>2</sub> fluxes in 2006 (Table 1c). It was because some of the nighttime  
485 chamber fluxes in warmer nights of summer 2006 were as large as the EC measured ecosystem  
486 net CO<sub>2</sub> fluxes corresponding to those same hours which could not be modelled to their full  
487 extent. RMSE lower than RMSRE meant the errors in modelling soil and understorey CO<sub>2</sub> fluxes  
488 were within the limit of random errors due to chamber measurements (Table 1c). It further  
489 indicated the robustness of modelled outputs for soil and understorey CO<sub>2</sub> fluxes under different  
490 WTD conditions (e.g., shallower in 2005 vs. deeper in 2006) (Table 1c).

491 **3.2. Seasonality in WTD and net ecosystem CO<sub>2</sub> exchange**

492       *Ecosys* simulated the seasonal and interannual variations in WTD from 2004 to 2009 well  
493 at the WPL (Figs. 3b, d, f, h, j, l) (Mezbahuddin et al., 2016). Seasonality in net CO<sub>2</sub> exchange at  
494 the WPL was predominantly governed by that in temperature which controlled the seasonality in  
495 phenology and GPP as well as that in  $R_e$ . *Ecosys* simulated the seasonality in phenology and  
496 hence GPP, and  $R_e$  well during a gradual growing season WTD drawdown from 2004 to 2009  
497 which was apparent by good agreements between modelled vs. EC-gap filled daily NEP (Fig. 3)  
498 and modelled vs. EC-measured hourly net CO<sub>2</sub> fluxes (Table 1). Modelled NEP throughout the

499 winters of most of the years were more negative than the EC-gap filled NEP indicating larger  
500 modelled CO<sub>2</sub> effluxes than EC-gap filled fluxes during the winter (Fig. 3). The onset of  
501 photosynthesis at the WPL varied interannually depending upon spring temperature which was  
502 also modelled well by *ecosys*. For instance, *ecosys* modelled a smaller early growing season  
503 (May) GPP and hence NEP in 2004 with a cooler spring than 2005 which was also apparent in  
504 daily EC-gap filled NEP (Figs. 3a vs. c).

505 **3.3. WTD effects on diurnal net ecosystem CO<sub>2</sub> exchange**

506 WTD variation can affect diurnal net CO<sub>2</sub> exchange by affecting peat O<sub>2</sub> status and  
507 consequently root and microbial O<sub>2</sub> and nutrient availability, growth and uptake thereby  
508 influencing CO<sub>2</sub> fixation and respiration. *Ecosys* simulated WTD effects on diurnal net CO<sub>2</sub>  
509 exchange at the WPL well over three 10-day periods with comparable weather conditions  
510 (radiation and air temperature) during late growing seasons (August) of 2005, 2006 and 2008  
511 (Fig. 4). A WTD drawdown from August 2005 to August 2006 in *ecosys* caused a reduction in  
512 peat water contents and a consequent increase in O<sub>2</sub> influxes from atmosphere into the peat that  
513 eventually caused an increase in modelled soil CO<sub>2</sub> effluxes (Fig. 5c). This stimulation of soil  
514 respiration was corroborated by modelled vs. chamber measured (Cai et al., 2010) night-time soil  
515 CO<sub>2</sub> fluxes and understorey autotrophic respiration ( $R_a$ ) in August 2006 with deeper WTD which  
516 were larger than those in 2005 with shallower WTD (Fig. 5b). Larger modelled soil CO<sub>2</sub> effluxes  
517 in 2006 contributed to the larger modelled ecosystem CO<sub>2</sub> effluxes ( $R_e$ ) that was also apparent in  
518 night-time EC CO<sub>2</sub> fluxes in 2006 which were larger than those in 2005 (Fig. 5a).

519 Continued WTD drawdown into the late growing season of 2008 (Fig. 4c) sustained  
520 improved peat oxygenation and hence larger modelled soil CO<sub>2</sub> effluxes (Fig. 5c). Consequently,  
521 modelled night-time net ecosystem CO<sub>2</sub> fluxes, and soil and understorey CO<sub>2</sub> fluxes in 2006 and

522 in 2008 were similarly larger than those in 2005 which was corroborated well by EC measured  
523 night-time fluxes during 2006 and 2008 vs. 2005 (Figs. 5a-b). Although night-time modelled and  
524 EC measured net ecosystem CO<sub>2</sub> fluxes in 2008 were larger than those in 2005, the day-time  
525 modelled and EC measured CO<sub>2</sub> fluxes in 2008 did not decline with respect to those in 2005  
526 (Fig. 5a). Similar day-time fluxes in 2005 and 2008 despite larger night-time fluxes in 2008 than  
527 in 2005 indicated a greater late growing season CO<sub>2</sub> fixation in 2008 with deeper WTD than in  
528 2005 with shallower WTD.

529 Beside WTD, temperature variation also profoundly affected ecosystem net CO<sub>2</sub>  
530 exchange at the WPL. For a given WTD condition warmer weather caused increases in  $R_e$  at the  
531 WPL (Figs. 4b-c and 5a-b). Night-time modelled, and EC and chamber measured ecosystem,  
532 soil, and understorey CO<sub>2</sub> fluxes, in warmer nights of day 214, 220 and 222 were larger than  
533 those in cooler nights of day 221, 224 and 218 in 2005, 2006 and 2008 respectively (Figs. 4b and  
534 5a-b). However, for a given temperature modelled and EC-gap filled night-time ecosystem CO<sub>2</sub>  
535 fluxes, and modelled and chamber measured night-time soil and understorey CO<sub>2</sub> fluxes were  
536 larger under deeper WT conditions in 2006 and 2008 than under shallower WT condition in 2005  
537 (denoted by the grey arrows in Figs. 4b and 5a-b). It showed net WTD drawdown effect on  $R_e$   
538 (separated from temperature effect) and hence on NEP.

539 The degree of  $R_e$  stimulation due to warming was also influenced by WTD at the WPL.  
540 The warming events in early to mid-August of 2006 and 2008, when WT was deeper than in late  
541 July of 2005, caused gradual increases in modelled, and EC and chamber measured night-time  
542 ecosystem, soil and understorey CO<sub>2</sub> effluxes (= $R_e$ ) (Figs. 6h, i, k, l). This  $R_e$  stimulation due to  
543 warming under deeper WT contributed to declines in modelled and EC-gap filled July-August  
544 NEP in 2006 and 2008 (Figs. 3e, i). Lack of similar stimulation in  $R_e$  with warming under

545 shallower WT in 2005 did not yield a similarly evident stimulation of either modelled or EC or  
546 chamber measured ecosystem, soil and understorey night-time CO<sub>2</sub> effluxes (Figs. 6g, j vs. h, i,  
547 k, l) which resulted in the absence of decline in July-August NEP as occurred in 2006 and 2008  
548 (Figs. 3c vs. e, i). Greater warming driven  $R_e$  stimulation under deeper WT further indicated the  
549 importance of WTD in mediating potential effects of future warmer climates on boreal peatland  
550 NEP.

### 551 **3.4. Interannual variations in WTD and net ecosystem productivity**

552 The effects of WTD drawdown on modelled and EC-gap filled diurnal net ecosystem  
553 CO<sub>2</sub> exchange also contributed to the effects of interannual variation in WTD on that of NEP.  
554 *Ecosys* simulated a site measured gradual drawdown of average growing season (May-August)  
555 WTD well from 2004 to 2009 (Fig. 7d) (Mezbahuddin et al., 2016). A small WTD drawdown  
556 simulated a large increase in growing season GPP from 2004 to 2005 as corroborated by similar  
557 increase in EC-derived GPP (Fig. 7b). This increase in GPP was also contributed by a larger GPP  
558 in May 2005 which was warmer than May 2004. This small WTD drawdown, however, did not  
559 raise either modelled or EC-derived growing season  $R_e$  from 2004 to 2005 (Fig. 7c). June and  
560 July of 2005 was cooler than 2004 by over 2°C which caused cooler soil that reduced  $R_e$  in 2005.  
561 Reduction in  $R_e$  in June-July 2005 due to cooler soil more than fully offset the increase in  $R_e$  due  
562 to the small WTD drawdown and resulted in modelled and EC-derived  $R_e$  that were smaller in  
563 the growing season of 2005 than in 2004 (Fig. 7c). Larger GPP and smaller  $R_e$  gave rise to  
564 modelled and EC-gap filled growing season NEP estimates that were larger in 2005 than those in  
565 2004 (Fig. 7a).

566 WTD drawdown from 2005 to 2006 raised both modelled and EC-derived growing  
567 season GPP and  $R_e$  (Figs. 7b-c). Warmer growing season in 2006 caused warmer soil that further

568 contributed to the increase in modelled and EC-derived growing season  $R_e$  from 2005 with  
569 shallower WT to 2006 with deeper WT (Figs. 5, 6 and 7c-d). An increase in growing season  $R_e$   
570 that was greater than the increase in growing season GPP caused a decline in modelled and EC-  
571 derived growing season NEP from 2005 to 2006 (Fig. 7a). Continued growing season WTD  
572 drawdown from 2006 to 2008 caused similar increases in modelled growing season GPP and  $R_e$   
573 and hence no significant change in modelled growing season NEP (Figs. 7a-d). With this  
574 continued WTD drawdown from 2006 to 2008, however, EC-derived growing season GPP  
575 increased more than EC-derived growing season  $R_e$  that resulted a larger EC-derived NEP in the  
576 growing season of 2008 than in 2006 (Figs. 7a-d). A further drawdown in WTD from the  
577 growing season of 2008 to that of 2009 caused reductions in both modelled and EC-derived  
578 growing season GPP and  $R_e$  (Figs. 7a-d). Reductions in GPP and  $R_e$  from 2008 to 2009 was also  
579 contributed by lower  $T_a$  in 2009 than in 2008 that caused cooler canopies and soil (Figs. 7b-d).  
580 The reduction in EC-derived growing season GPP was larger than that in EC-derived growing  
581 season  $R_e$  thereby causing a decrease in growing season EC-gap filled NEP from 2008 to 2009  
582 (Figs. 7a- c). On the contrary, the reduction in modelled growing season GPP was smaller than  
583 the reduction in modelled  $R_e$  that yielded an increase in modelled growing season NEP from  
584 2008 to 2009 (Figs. 7a-c).

585 Modelled and EC-derived estimates of growing season GPP and  $R_e$  in 2009 were larger  
586 than those in 2004 despite similar mean  $T_a$  in those years (Figs. 7a-d). It suggested that increases  
587 in growing season GPP and  $R_e$  from 2004 to 2009 was a net effect of the deepening of average  
588 growing season WT (Figs. 7a-d). It was further corroborated by polynomial regressions of  
589 modelled growing season estimates of GPP and  $R_e$  against modelled average growing season  
590 WTD, and similar regressions of EC-derived growing season GPP and  $R_e$  against site measured

591 average growing season WTD (Figs. 8a-c). These relationships showed that there were increases  
592 in modelled and EC-derived growing season GPP and  $R_e$  with deepening of the growing season  
593 WT from 2004 to 2008 after which further WTD drawdown in 2009 started to cause slight  
594 declines in both GPP and  $R_e$  (Figs. 8b-c). Neither modelled nor EC-gap filled estimates of  
595 growing season NEP yielded significant regressions when regressed against modelled and  
596 measured growing season WTD respectively (Fig. 8a). It indicated that similar increases in  
597 modelled and EC-derived growing season estimates of GPP and  $R_e$  with deepening of WT left no  
598 net effects of WTD drawdown on either modelled or EC-derived growing season NEP (Figs. 7a-  
599 d and 8a).

600 Similar to the growing season trend, drawdown of both measured and modelled WTD  
601 averaged over the ice free periods (May-October) from 2004 to 2008 generally stimulated annual  
602 modelled and EC-derived GPP and  $R_e$  (Figs. 7f, g, h and 8e, f). Similar increases in both  
603 modelled and EC-derived annual GPP and  $R_e$  with WTD drawdown left no net WTD effects on  
604 modelled and EC-gap filled annual NEP (Figs. 7e, 8d). Although modelled WTD effects on GPP,  
605  $R_e$  and hence NEP corroborated well by EC-derived GPP,  $R_e$  and EC-gap filled NEP, the  
606 modelled values for growing season and annual GPP and  $R_e$  were consistently higher than the  
607 EC-derived estimates of those throughout the study period (Figs. 7b, c, f, g and 8b, c, e, f).

608 Increased GPP with WTD drawdown (Figs. 7b, f and 8b, e) was modelled predominantly  
609 through increased root growth and uptake of nutrients and consequently improved leaf nutrient  
610 status and hence more rapid CO<sub>2</sub> fixation in vascular PFTs. Under shallow WT during the  
611 growing season of 2004, roots in modelled black spruce and tamarack PFTs hardly grew below  
612 0.35 m from the hummock surface. Modelled root densities of both black spruce and tamarack  
613 were higher by 2-3 orders of magnitude in the top 0.19 m of the hummock (data not shown). A

614 WTD drawdown by 0.35 m from the growing season of 2004 to that of 2009 caused increase in  
615 maximum modelled rooting depth in both PFTs (Table 2). Increased root growth in modelled  
616 vascular PFTs augmented root surface area for nutrient uptake under deeper WT in the growing  
617 season of 2009 than in 2004. Increased root surface area along with increased nutrient  
618 availability due to more rapid mineralization with improved aeration as a result of WTD  
619 drawdown from 2004 to 2009 caused improved root nutrient uptake in modelled vascular PFTs.  
620 Increased root growth, nutrient availability and hence uptake due to WTD drawdown from the  
621 growing season of 2004 to that of 2009 caused an increase in modelled foliar N concentrations in  
622 black spruce, tamarack and dwarf birch PFTs driving the increases in GPP modelled over this  
623 period (Figs. 7b, f and 8b, e) (Table 2).

624 **3.5. Simulated drainage effects on WTD and NEP**

625 Artificial drainage can drastically alter WTD in a peatland that can cause dramatic  
626 changes in peatland NEP by shifting the balance between GPP and  $R_e$ . Projected growing season  
627 WT was deeper by ~0.5 m and ~0.55 m respectively from those in the real-time simulation in  
628 drainage cycles 1 and 2 in all the years from 2004 to 2009 (Fig. 9a). Modelled growing season  
629 GPP increased with drainage-induced WTD drawdown up to ~0.5 m below the hollow surface  
630 (~0.8 m below the hummock surface) below which GPP decreased (Figs. 9c, f). The WTD  
631 drawdown affected modelled vascular and non-vascular growing season GPP quite differently.  
632 Modelled growing season vascular GPP increased with WTD drawdown before it plateaued and  
633 eventually decreased when WTD fell below ~0.6 m from the hollow surface (~0.9 m below the  
634 hummock surface) (Figs. 10a, c, e). On the contrary, modelled non-vascular growing season GPP  
635 continued to decrease with WTD drawdown below ~0.1 m from the hollow surface (~0.4 m  
636 below the hummock surface) (Figs. 10a-b, d).

637                    WTD drawdown due to simulated drainage not only affected modelled growing season  
638                    GPP but also affected, and was affected by, the associated change in transpiration from vascular  
639                    canopies. Deeper WTD<sub>x</sub> in drainage cycle 1 caused larger hydraulic gradients and greater lateral  
640                    discharge thereby deepening the WT with respect to that in the real-time simulation (Figs. 9a).  
641                    Larger GPP throughout the growing seasons of 2004-2007 in the drainage cycle 1 than in the  
642                    real-time simulation caused a greater vertical water loss through rapid transpiration from  
643                    vascular canopies that further contributed to this deepening of WT (Fig. 9c). However, greater  
644                    lateral water discharge in drainage cycle 2 caused by deeper WTD<sub>x</sub> did not deepen the modelled  
645                    growing season WT much below that in cycle 1 (Fig. 9a). The larger lateral water loss through  
646                    discharge in drainage cycle 2 than in cycle 1 was mostly offset by slower vertical water losses  
647                    due to vascular plant water stress as indicated by smaller GPP in the drainage cycle 2 (Fig. 9c).  
648                    The changing feedbacks between WTD, and GPP and plant water relations in *ecosys* also  
649                    indicated the ability of the model to simulate hydrological self-regulation which is an important  
650                    characteristic of peatland eco-hydrology (Dise, 2009).

651                    Modelled growing season  $R_e$  continued to increase with projected drainage driven WTD  
652                    drawdown (Figs. 9d, g). Reductions in modelled growing season  $R_e$  from drainage cycle 1 to 2  
653                    during 2006-2009 indicated  $R_e$  inhibition due to desiccation of near surface peat layers and  
654                    surface residues (Fig. 9d). Overall GPP increased more than  $R_e$  with drainage driven initial WTD  
655                    drawdown that caused a small increase in modelled growing season NEP (Figs. 9 b, e).  
656                    Continued drainage driven WTD drawdown, however, caused declines in GPP particularly in  
657                    model years of 2008 and 2009 (Figs. 9c). This decrease in GPP was also accompanied by  
658                    increased  $R_e$  thereby causing a decrease in NEP when WT fell below a threshold of about ~0.45  
659                    m from the hollow surface, particularly during the drier years (Figs. 9b-g). This projected

660 drainage effect on WTD and NEP may be transient. Long-term manipulation of WTD may  
661 produce different trajectories of WTD effects on C processes and plant water relations in  
662 northern boreal peatlands via vegetation adaptation and succession (Strack et al., 2006; Munir et  
663 al., 2014).

664 **4. Discussion**

665 **4.1. Modelling WTD effects on northern boreal peatland NEP**

666 Hourly modelled, EC measured, and chamber measured net ecosystem, and soil and  
667 understorey CO<sub>2</sub> fluxes, and modelled and EC-derived seasonal and annual NEP, GPP and  $R_e$   
668 estimates showed that WTD drawdown raised both GPP and  $R_e$  at the WPL (Figs. 3-8). Similar  
669 increases in GPP and  $R_e$  with WTD drawdown yielded no net effect of WTD drawdown on NEP  
670 at the WPL during 2004-2009 (Figs. 7-8). Four central hypotheses which outlined how coupled  
671 eco-hydrology and biogeochemistry algorithms in *ecosys* would simulate and explain the  
672 mechanisms of these WTD effects on  $R_e$ , GPP and NEP at the boreal fen peatland under study  
673 are examined in details in the following sections of 4.1.1 to 4.1.4.

674 **4.1.1. Hypothesis 1: Increase in  $R_e$  with WTD drawdown**

675 Shallow WTD in *ecosys* caused shallow aerobic zone above WT and thicker anaerobic  
676 zone below the WT. In the shallow aerobic zone, peat O<sub>2</sub> concentration [O<sub>2s</sub>] was well above the  
677 Michaelis-Menten constant for O<sub>2</sub> reduction ( $K_m=0.064$  g m<sup>-3</sup>) and hence DOC oxidation and  
678 consequent microbial uptake and growth in *ecosys* was not much limited by [O<sub>2s</sub>] (Eqs. A17a,  
679 C14c). On the contrary, [O<sub>2s</sub>] in the thicker anaerobic zone below the WT was well below  $K_m$  so  
680 that DOC oxidation was coupled with DOC reduction by anaerobic heterotrophic fermenters,  
681 which yielded much less energy (4.4 kJ g<sup>-1</sup> C) than did DOC oxidation coupled with O<sub>2</sub>  
682 reduction (37.5 kJ g<sup>-1</sup> C) (Fig. 1) (Eq. A21). Lower energy yields in the thicker anaerobic zone

683 resulted in slower microbial growth (Eq. A25) and  $R_h$  (Eq. A13). Since the anaerobic zone in  
684 *ecosys* was thicker than the aerobic zone under shallow WT, lower modelled  $R_h$  in the anaerobic  
685 zone contributed to reduced modelled soil respiration and hence  $R_e$  that was corroborated by EC  
686 and chamber measurements at the WPL (Figs. 5-8) (Tables 1 and 2).

687 WTD drawdown in *ecosys* caused peat pore drainage and increased  $\theta_g$  thereby deepening  
688 of the aerobic zone. It raised  $D_g$  (Eq. D44) and increased  $O_2$  influxes into the peat (Fig. 5c) (Eqs.  
689 D42-D43). Increased  $O_2$  influxes enhanced  $[O_{2s}]$  and stimulated  $R_h$  (Eqs. A13, A20), soil  
690 respiration and hence  $R_e$  (Figs. 5-8). Rapid mineralization of DON and DOP due to improved  
691  $[O_{2s}]$  under deeper WT also raised aqueous concentrations of  $NH_4^+$ ,  $NO_3^-$  and  $H_2PO_4^-$  (Eqs.  
692 C23a, c, e) that increased microbial nutrient availability, uptake (Eq. A22) and growth (Eq. A29)  
693 and further enhanced  $R_e$  (Fig. 1) (Figs. 5-8). Modelled  $R_e$  stimulation by improved peat  
694 oxygenation due to WTD drawdown was corroborated well by EC and chamber measurements at  
695 the site (Figs. 5-8) (Tables 1 and 2). However, the chamber measured nighttime net  $CO_2$  fluxes  
696 during warmer nights of 2006 with deeper WT were sometimes as large as corresponding EC-  
697 measured net ecosystem  $CO_2$  fluxes (Figs. 5-6). Those very large chamber  $CO_2$  effluxes could  
698 not be modelled to their full extent and consequently modelled vs. chamber  $CO_2$  flux regression  
699 yielded a slope lower than  $1\pm0.1$  in 2006 (Table 1c). Although modelled rate of increase in  $R_e$   
700 with each 0.1 m of WTD drawdown was larger than EC-derived rate, it is still comparable with  
701 rates reported for other similar peatlands (Table 2). Kotowska (2013) carried out chamber based  
702 field measurements and laboratory incubation experiments in a moderately rich fen very close to  
703 our study site which reported that a WTD drawdown driven stimulation of aerobic microbial  
704 decomposition contributed to increased  $R_e$ . Mäkiranta et al. (2009) also found rapid microbial

705 decomposition in a Finish peatland due to thicker aerobic zone and consequently larger amounts  
706 of decomposable organic matter exposed to aerobic oxidation.

707 Apart from WTD, peat warming in *ecosys* also increased rates of decomposition (Eq. A1)  
708 through an Arrhenius function (Eq. A6) and increased  $R_h$  and  $R_e$  (Figs. 4-7). Warming effect on  
709 decomposition in *ecosys* was also modified by WTD. For a similar warming, greater thermal  
710 diffusivity in peat with deeper WT and consequent smaller water contents caused greater peat  
711 warming (Eqs. D34, D36). It enabled larger simulation of  $R_e$  during warming periods in 2006  
712 and 2008 with deeper WT than in 2005 (Fig. 6). Increased stimulation of peat decomposition by  
713 warming under deeper WT was also modelled by Grant et al. (2012) using the same model  
714 *ecosys* over a northern fen peatland at Wisconsin, USA and by Ise et al. (2008) using a land  
715 surface scheme named ED-RAMS (Ecosystem Demography Model version 2 integrated with the  
716 Regional Atmospheric Modeling System) coupled with a soil biogeochemical model across  
717 several shallow and deep peat deposits in Manitoba, Canada.

718 **4.1.2. Hypothesis 2: Increase in GPP with WTD drawdown**

719 Modelled WTD variations influenced GPP by controlling root and microbial O<sub>2</sub>  
720 availability, energy yields, root and microbial growth and decomposition, rates of mineralization  
721 and hence root nutrient availability and uptake (Fig. 1). Wet soils under shallow WT caused low  
722 O<sub>2</sub> diffusion (Fig. 5c) (Eqs. D42-D44) into the peat and consequent low [O<sub>2s</sub>] meant that root O<sub>2</sub>  
723 demand had to be mostly met by [O<sub>2r</sub>]. *Ecosys* inputs for root porosity ( $\theta_{pr}=0.1$ ) that governed  
724 O<sub>2</sub> transport through aerenchyma (Eq. D45) and hence maintained [O<sub>2r</sub>] was not enough to meet  
725 the root O<sub>2</sub> demand in saturated soil by the two over-storey tree PFTs i.e. black spruce and  
726 tamarack, causing shallow root systems to be simulated in these two tree PFTs under shallow  
727 WTD (Sec. 3.4). The under-storey shrub PFT (dwarf birch) had a higher root porosity ( $\theta_{pr}=0.3$ )

728 and hence had deeper rooting under shallow WT than the two tree PFTs (Sec. 3.4). Shallow  
729 rooting in the tree PFTs reduced root surface area for nutrient uptake. Root nutrient uptake (Eqs.  
730 C23b, d, f) in all the PFTs was also constrained by low nutrient availability due to smaller  
731 aqueous concentrations of  $\text{NH}_4^+$ ,  $\text{NO}_3^-$  and/or  $\text{H}_2\text{PO}_4^-$  (Eqs. C23a, c, e) resulting from slower  
732 mineralization (Eq. A26) of DON and DOP (Eq. A7) because of low  $[\text{O}_{2s}]$  in the wet soils under  
733 shallow WT (Fig. 1). Slower root growth and nutrient uptake caused lower foliar  $\sigma_N$  and/or  $\sigma_P$   
734 with respect to foliar  $\sigma_C$  (Eq. C11) that slowed the rates of carboxylation (Eq. C6) and hence  
735 reduced vascular GPP (Eq. C1) under shallow WT.

736 WTD drawdown enhanced  $\text{O}_2$  diffusion (Fig. 5c) (Eqs. D42-D44) and raised  $[\text{O}_{2s}]$  so that  
737 root  $\text{O}_2$  demand in all the three vascular PFTs was almost entirely met by  $[\text{O}_{2s}]$ . Consequently  
738 roots in all the PFTs could grow deeper which increased the root surface for nutrient uptake  
739 (Table 2) (Sec. 3.4). Increase in modelled rooting depth due to WTD drawdown was  
740 corroborated well by studies on same PFTs as in our study grown on similar peatlands very close  
741 to the study site (Table 2). Murphy et al. (2009) found a significant increase in tree fine root  
742 production with WTD drawdown by 0.15-0.2 m during a WTD manipulation study in a Finish  
743 peatland. Beside improved root growth, greater  $[\text{O}_{2s}]$  under deeper WT also enhanced rates of  
744 mineralization (Eq. A26) of DON and DOP (Eq. A7) that raised aqueous concentrations of  $\text{NH}_4^+$ ,  
745  $\text{NO}_3^-$  and/or  $\text{H}_2\text{PO}_4^-$  and hence facilitated root nutrient availability and uptake (Fig. 1). Enhanced  
746 root nutrient uptake increased foliar  $\sigma_N$  and/or  $\sigma_P$  with respect to foliar  $\sigma_C$  (Eq. C11) that  
747 hastened the rates of carboxylation (Eq. C6) and hence raised vascular GPP (Eq. C1) under  
748 deeper WT.

749 The three modelled vascular PFT were predominantly N limited as indicated by mass-  
750 based modelled foliar N to P ratios that matched well with site-measured mass-based foliar N to

751 P ratios (Table 2). Mass-based modelled and measured foliar N to P ratio in all the PFTs were  
752 less than 16:1 indicating that the vegetation at the WPL was N limited (Aerts and Chapin III,  
753 1999). Since the modelled PFTs were predominantly N limited, increases in foliar N  
754 concentrations as a result of improved root nutrient availability, growth and nutrient uptake with  
755 WTD drawdown enhanced modelled carboxylation rates and hence modelled GPP. In a similar  
756 fen peatland close to our study site, Choi et al. (2007) found an increase in peat  $\text{NO}_3^-$ -N due to  
757 enhanced mineralization and nitrification stimulated by a WTD drawdown which improved  
758 foliar N status, and hence increased radial tree growth of black spruce and tamarack (Table 2).  
759 Macdonald and Lieffers (1990) also found improved foliar N concentrations in black spruce and  
760 tamarack trees that enhanced net photosynthetic C assimilation rates by those tree species in a  
761 northern Alberta moderately rich fen (Table 2). The rates of increases in foliar N concentrations  
762 in black spruce and tamarack trees due to WTD drawdown as reported in those studies are  
763 comparable with those in our modelled outputs (Table 2). Although modelled rate of increase in  
764 GPP with each 0.1 m of WTD drawdown was larger than EC-derived rate, it is still comparable  
765 with rates reported for other similar peatlands (Table 2).

#### 766 **4.1.3. Hypothesis 3: Microbial water stress on $R_e$ due to WT deepening below a threshold**

##### 767 **WTD**

768 When modelled WTD fell below a threshold of ~0.3 m from the hollow surface (~0.6 m  
769 below the hummock surface), desiccation of the surface residue layer and near surface shallow  
770 peat layers reduced microbial access to substrate for decomposition (Eq. A15) which enabled  
771 simulation of reduced  $R_h$  in those layers. When reduction in surface residue and near-surface  $R_h$   
772 more than fully offset the increase in deeper  $R_h$ , net ecosystem  $R_h$  decreased. The offsetting  
773 effect on  $R_h$  partly contributed to simulated decrease in growing season  $R_e$  ( $=R_h+R_a$ ) from 2008

774 to 2009 with WTD drawdown that was corroborated by a similar decrease in EC-derived  $R_e$  (Fig.  
775 7c). Greater reductions in  $R_h$  in desiccated surface residue and near surface peat layers also  
776 caused the reductions in growing season  $R_e$  in drainage cycle 2 from those in cycle 1 during  
777 2007-2009 in the simulated drainage study (Fig. 9d). Similar to our study, Peichl et al. (2014)  
778 found reductions in  $R_e$  when WTD fell below a threshold of 0.25 m from the peat surface in a  
779 Swedish fen which could be partially attributed to reduction in near surface  $R_h$  due to  
780 desiccation. Mettrop et al. (2014) in a controlled incubation experiment found that the rates of  
781 microbial respiration in a nutrient rich Dutch fen initially increased with peat drying and  
782 consequent improved aeration. But excessive drying and consequent peat desiccation in their  
783 study reduced microbial respiration efficiency, growth and biomass. Dimitrov et al. (2010a)  
784 while modelling CO<sub>2</sub> exchange of a northern temperate bog using *ecosys* showed that a decrease  
785 in desiccated near surface peat respiration partially offset increased deeper peat respiration when  
786 WT deepened below a threshold of 0.6-0.7 m from the hummock surface.

787 **4.1.4. Hypothesis 4: Plant water stress on GPP due to WT deepening below a threshold**

788 **WTD**

789 Modelled WTD drawdown below a threshold level also caused rapid peat pore drainage  
790 and low moisture contents in the near surface peat layers which were colonized by most of the  
791 vascular root systems and all of the belowground biomasses of non-vascular mosses (Eqs. D9-  
792 D29). When WTD fell below ~0.1 m from the hollow surface (~0.4 m below the hummock  
793 surface), vertical recharge through capillary rise from the WT was not adequate to maintain near  
794 surface peat moisture. It reduced peat water potential ( $\psi_s$ ) and raised peat hydraulic resistance  
795 ( $\Omega_s$ ) (Eq. B9) that suppressed root and moss water uptake ( $U_w$ ) (Eq. B6) from desiccated near  
796 surface peat layers (Fig. 1). Since moss  $U_w$  entirely depended upon moisture supply from the

797 near surface layers, reduction in  $U_w$  from desiccation of these layers caused reduction in moss  
798 canopy water potential ( $\psi_c$ ) and hence moss GPP (Fig. 1) (Eqs. C1, C4) (Mezbahuddin et al.,  
799 2016). Reduction in root  $U_w$  from desiccated near surface layers, however, was offset by  
800 increased root  $U_w$  (Eq. B6) from deeper wetter layers, which had higher  $\psi_s$  and lower  $\Omega_s$ , due to  
801 deeper root growth facilitated by enhanced aeration. It enabled the vascular PFTs in *ecosys* to  
802 sustain  $\psi_c$ , canopy turgor potential ( $\psi_t$ ) (Eq. B4), stomatal conductance ( $g_c$ ) (Eqs. B2, C4) and  
803 hence to sustain increased GPP (Eq. C1) due to higher root nutrient availability and uptake (Fig.  
804 1) (Mezbahuddin et al., 2016). Increased vascular GPP and consequent greater vascular plant  
805 growth further imposed limitations of water, nutrient and light to the modelled non-vascular  
806 PFTs due to interspecific competition and greater shading from the overstorey vascular PFTs.  
807 However, increases in vascular GPP due to enhanced plant nutrient status more than fully offset  
808 the suppression in moss GPP due to moss drying, and greater shading and competition from the  
809 overstorey, thereby causing a net increase in modelled GPP with WTD drawdown (Figs. 7b and  
810 10b-c). This simulation of increased vascular dominance over moss with deepening of WT was  
811 corroborated by several WTD manipulation studies (e.g., Moore et al., 2006, Munir et al., 2014)  
812 in similar peatlands in Alberta that reported increased tree, shrub and herb growths over mosses  
813 with WTD drawdown. However, increase in projected vascular GPP eventually plateaued and it  
814 started to decline when WT fell below ~0.6 m from the hollow surface (~0.9 m below the  
815 hummock surface) (Figs. 10c, e). It was because deeper root  $U_w$  (Eq. B6) could no longer offset  
816 suppression of near-surface root  $U_w$  when WT fell below threshold WTD, thereby causing lower  
817  $\psi_c$ ,  $\psi_t$  (Eq. B4),  $g_c$  (Eqs. B2, C4) and slower CO<sub>2</sub> fixation (Eq. C6) (Fig. 1).

818 These threshold WTD effects on modelled vascular and non-vascular plant water  
819 relations were validated well by testing modelled vs. site measured hourly energy fluxes (latent

820 and sensible heat) and Bowen ratios, and modelled vs. site measured daily soil moisture at  
821 different depths throughout 2004-2009 as described in Mezbahuddin et al. (2016). Riutta et al.  
822 (2007) measured a reduction in moss productivity due to water limitation when WTD fell below  
823 ~0.15 m from the surface in a Finish fen peatland. However, they reported a sustained vascular  
824 GPP during that period indicating no vascular water stress (Riutta et al., 2007). Peichl et al.  
825 (2014) measured a reduction in moss GPP due to moss drying caused by insufficient moisture  
826 supply through capillary rise when WTD fell below 0.25 m from the surface in a Swedish fen.  
827 Reductions in moss GPP due to decreased moss canopy water potentials were also modelled by  
828 Dimitrov et al. (2011) using the same model *ecosys* when WTD fell below 0.3 m from the  
829 hummock surface of a Canadian temperate bog. They, however, found no vascular plant water  
830 stress and hence no reduction in vascular GPP during that period. Similarly, Kuiper et al. (2014)  
831 found reductions in moss productivity with peat drying while vascular productivity sustained in a  
832 simulated drought experiment on a Danish peat.

833 Continued deepening of WT can also cause vascular plant water stress and hence  
834 reductions in vascular GPP as projected in our drainage simulation (Figs. 10c, e). It can also be  
835 corroborated by field measurements across various northern boreal fen peatlands in Canada and  
836 Sweden. Sonnentag et al. (2010) found a reduction in stomatal conductance ( $g_c$ ) of a canopy that  
837 included tamarack and dwarf birch and a consequent decline in GPP when WT fell below 0.3 m  
838 from the ridge surface at a fen peatland in Saskatchewan. Peichl et al. (2014) also found a  
839 reduction in vascular GPP due to plant water stress when WTD fell below 0.25 m from the  
840 surface in a Swedish fen. The WTD threshold for reductions in vascular GPP in those two field  
841 studies were shallower than that in our modelled projection i.e. ~0.6 m from the hollow surface  
842 (~0.9 m below the hummock surface) (Figs. 10a, c, e) thereby indicating different vertical

843 rooting patterns determined by specific interactions between hydrologic properties and rooting.  
844 Lafleur et al. (2005) and Schwärzel et al. (2006) found much deeper WTD thresholds for  
845 reductions in vascular transpiration that could negatively affect vascular GPP over a Canadian  
846 pristine bog and a German drained fen respectively. Those WTD thresholds were ~0.65 and ~0.9  
847 m below the surface for the pristine and drained peatland respectively, further indicating the  
848 importance of root-hydrology interactions and the resultant root adaptations, growth and uptake  
849 in determining WTD effects on vascular GPP across peatlands.

850 **4.2. Divergences between modelled and EC-derived annual GPP,  $R_e$  and NEP**

851 Modelled seasonal and annual GPP and  $R_e$  were consistently larger than EC-derived  
852 estimates of GPP and  $R_e$  during 2004-2009 (Figs. 7b, c, f, g). Although modelled annual GPP  
853 and  $R_e$  were larger than the EC-derived estimates, modelled annual NEP were consistently lower  
854 than the EC gap-filled annual NEP (Fig. 7e). Modelled annual NEP were smaller than EC-  
855 derived estimates because modelled  $R_e$  were larger than EC-derived estimates by margins bigger  
856 than by what modelled GPP were larger than EC-derived estimates (Figs. 7f-g). Modelled  $R_e$   
857 were larger than EC-derived  $R_e$  estimates mainly due to the presence of gap filled night-time CO<sub>2</sub>  
858 fluxes ( $=R_e$ ) in EC-derived estimates which were smaller than corresponding modelled values. It  
859 was apparent in negative intercepts that resulted from regressions of modelled vs. gap-filled net  
860 CO<sub>2</sub> fluxes (Table S1 in supplementary material). Gap filled  $R_e$  fluxes were calculated from soil  
861 temperature ( $T_s$ ) at a shallow depth (0.05 m) (Sec. 2.2.2). During night-time and in the winter,  
862 peat at this shallow depth rapidly cooled down and yielded smaller night-time gap-filled CO<sub>2</sub>  
863 fluxes (Figs. 3, 5 and 6). On the contrary, corresponding modelled CO<sub>2</sub> effluxes were affected by  
864 not only the cooler shallow peat layers but also the warmer deeper peat layers and thus were  
865 larger than the gap-filled fluxes (e.g., Figs. 5a, 6h-i). Like modelled CO<sub>2</sub> effluxes, chamber

866 measured CO<sub>2</sub> effluxes in cooler nights also did not decline as rapidly as did the corresponding  
867 gap-filled CO<sub>2</sub> fluxes as night progressed which further indicated the likely contribution of gap-  
868 filling artifact to CO<sub>2</sub> effluxes that were smaller than corresponding modelled fluxes (e.g., Figs.  
869 5b vs. a, 6j-k vs. g-h).

870 Systematic uncertainties embedded in EC methodology could also have contributed to  
871 EC-derived annual and growing season  $R_e$  estimates which were smaller than the modelled  
872 values (Figs. 7c, g). The major uncertainty in the EC methodology is the possible  
873 underestimation of nighttime EC CO<sub>2</sub> flux measurements due to poor turbulent mixing under  
874 stable air conditions (Goulden et al., 1997; Miller et al., 2004). On the contrary, modelled  
875 biological production of CO<sub>2</sub> by plant and microbial respiration was independent of turbulent  
876 mixing which could thus contribute to modelled  $R_e$  that were larger than EC-derived estimates.

877 Complete energy balance closure in the model as opposed to incomplete (~75%) energy  
878 balance closure in EC measurements would also give rise to modelled evapotranspiration and  
879 GPP values that were larger than EC-derived estimates (Figs. 7b, f) (Mezbahuddin et al., 2016).  
880 Modelled GPP influenced modelled  $R_e$  through root exudation and litter fall (Fig. 1). Therefore,  
881 modelled GPP that were larger than EC-derived estimates would have further contributed to  
882 modelled growing season and annual  $R_e$  estimates that were larger than EC-derived estimates  
883 (Figs. 7c, g).

884 Modelled GPP and hence  $R_e$  can also be larger than EC-derived estimates due to  
885 uncertainties in model inputs for soil organic N, N deposition, N<sub>2</sub> fixation and any other sources  
886 of N inputs into the modelled ecosystem. In *ecosys*, plant productivity is governed by foliar N  
887 status which is constrained by root N availability and uptake. Our input for organic N into each  
888 modelled peat layer was measured for corresponding depth at the site (Fig. 2). To simulate N

889 deposition, background wet deposition rates of 0.5 mg ammonium-N, and 0.25 mg nitrate-N per  
890 litre of precipitation which were reported for the study area were used as model inputs. However,  
891 from visual field observations, it was evident that there was a significant amount of nutrient  
892 inflow with the lateral water influxes into this fen peatland from the surrounding upland forests  
893 which was not quantified. To mimic this lateral nutrient inflow, we doubled the background wet  
894 deposition of  $\text{NH}_4^+$  and  $\text{NO}_3^-$  as reported for the area and used these as surrogates of lateral  
895 nutrient inflow into the modelled ecosystem. *Ecosys* also included a  $\text{N}_2$  fixing algorithm which  
896 simulated symbiotic  $\text{N}_2$  fixation in moss canopies that was reported for the boreal forests (Sec.  
897 2.2.3). We tested the adequacy of these N inputs into the model by comparing modelled leaf N  
898 concentrations against those measured in the field. The modelled foliar N concentrations for the  
899 vascular PFTs corroborated well against site measurements (Table 2). To further examine the  
900 contribution of uncertainty due to model inputs towards the divergence between modelled and  
901 EC-derived seasonal and annual GPP and  $R_e$ , we performed a sensitivity test where we had a  
902 parallel run without doubling the background N wet deposition rates in the model, hence  
903 simulating no lateral N influx into the modelled ecosystem. Unlike the run with lateral N inflow,  
904 the parallel run without lateral N inflow simulated GPP and  $R_e$  which were very close to the EC-  
905 derived estimates. However, the regressions between hourly modelled net  $\text{CO}_2$  fluxes from the  
906 parallel run and EC-measured hourly net  $\text{CO}_2$  fluxes gave slopes of  $\sim 0.8$  indicating under-  
907 simulation of the EC-measured fluxes in the parallel run with no lateral N inflow.

908 **5. Conclusions**

909 Our modelling study showed that, when adequately coupled into algorithms of a process-  
910 based ecosystem model, the existing knowledge of peatland eco-hydrological and peat  
911 biogeochemical processes could explain underlying mechanisms that governed WTD effects on

912 net ecosystem CO<sub>2</sub> exchange of a boreal fen. Testing of our hypotheses against EC-measured net  
913 CO<sub>2</sub> fluxes, automated chamber fluxes and other biometric measurements at the site revealed that  
914 a drier weather driven WTD drawdown at this boreal fen raised both  $R_e$  and GPP due to  
915 improved aeration that facilitated 1) microbial and root O<sub>2</sub> availability, energy yields, growth and  
916 decomposition which raised microbial and root respiration; and 2) rapid nitrogen mineralization,  
917 and consequently increased root nitrogen availability and uptake that improved leaf nitrogen  
918 status and hence raised carboxylation (Figs. 1, 7-8) (Table 2). Similar increases in  $R_e$  and GPP  
919 with WTD drawdown to a certain depth caused no net WTD drawdown effect on NEP (Fig. 8).  
920 Modelled drainage projection, however, showed that further WTD drawdown caused by either  
921 drainage or climate change induced drying would cause plant water stress and reduce GPP and  
922 hence NEP of this boreal fen (Figs. 9-10). This study further reconciled and mechanistically  
923 explained the WTD effects on seasonal and annual GPP,  $R_e$  and hence NEP of this boreal fen  
924 which was previously speculated from EC-derived estimates. However, although modelled CO<sub>2</sub>  
925 fluxes were validated well by the EC and chamber measured net CO<sub>2</sub> fluxes, modelled values of  
926 annual and seasonal GPP and  $R_e$  were consistently larger than the EC-derived estimates (Table 1)  
927 (Figs. 7-8) (Sec. 4.2). These discrepancies between modelled and EC-derived GPP and  $R_e$   
928 estimates also raised a potential research question of whether or not to use more robust process-  
929 based estimates of these peatland C balance components instead of empirically modelled EC-  
930 derived estimates that might not include some of the above discussed offsetting feedbacks in  
931 peatland eco-hydrology and biogeochemistry.

932 The model algorithms that were used in this study represented coupled feedbacks among  
933 ecosystem processes that governed carbon, water, energy, and nutrient (N, P) cycling in a  
934 peatland ecosystem. These feedbacks were thus not parameterized for this particular boreal fen

935 peatland site. Instead, the modelled boreal fen was simulated from peatland specific model inputs  
936 for weather, soil, and vegetation properties that had physical meaning and were quantifiable at  
937 the site (Fig. 2). These modelled process level interactions were also validated by corroborating  
938 modelled outputs against site measurements. On the contrary, most of the current peatland C  
939 models use scalar functions to represent these feedbacks and so those model algorithms have to  
940 be parameterized for each peatland site. Therefore, the modelling approach as described in this  
941 study should be more robust than the scalar feedback approach while assessing WTD effects on  
942 peatland C balance under contrasting peat types, climates and hydrology, or under unknown  
943 future climates. These process level feedbacks are also scalable once the peatlands of interest are  
944 defined within the modelled landscapes by scalable model inputs for weather; peat hydrological,  
945 physical, and biological properties; and plant functional types (Sec. 2.2.3). Current global land  
946 surface models either lack or have very poor representation of these feedbacks which is thus far  
947 limiting our large scale predictive capacity on WTD effects on boreal peatland C stocks. This  
948 modelling exercise would thus provide valuable information to improve representation of these  
949 feedbacks into next generation land surface models. Therefore, the insights gained from this  
950 modelling study should be a significant contribution to our understanding and apprehension of  
951 how peatlands would behave with changing hydrology under future drier and warmer climates.

952      **Code availability**

953            The *ecosys* model codes are listed in equation forms and sufficiently described in the  
954            supplementary material. The model codes that were written in FORTRAN will also be available  
955            on request from either [symon.mezbahuddin@gov.ab.ca](mailto:symon.mezbahuddin@gov.ab.ca) or [rgrant@ualberta.ca](mailto:rgrant@ualberta.ca).

956 **Data availability**

957 Field data that were used to validate model outputs are available at

958 <http://fluxnet.ornl.gov/site/292>.

959 **Author contribution**

960 M. Mezbahuddin contributed to the model code modification and development, designing  
961 modelling experiment, simulation, validation, and analyses of modelled outputs. R. F. Grant is  
962 the original developer of the model *ecosys* and also contributed into simulation design and model  
963 runs. L. B. Flanagan was site principal investigator who led the collection, and quality control of  
964 the field data that were used to validate model outputs. M. Mezbahuddin wrote the manuscript  
965 with significant contributions from R. F. Grant and L. B. Flanagan.

966 **Acknowledgments**

967 Computing facilities for the modelling project was provided by Compute Canada,  
968 Westgrid, and University of Alberta. Funding for the modelling project was provided by several  
969 research awards from Faculty of Graduate Studies and Research and Department of Renewable  
970 Resources of University of Alberta and a Natural Sciences and Engineering Research Council  
971 (NSERC) of Canada discovery grant. The field research was carried out as part of the Fluxnet-  
972 Canada Research Network and the Canadian Carbon Program and was funded by grants to  
973 Lawrence B. Flanagan from NSERC, Canadian Foundation for Climate and Atmospheric  
974 Sciences, and BIOCAP Canada.

975 **References**

976 Aerts, R. and Chapin III, F.: The mineral nutrition of wild plants revisited: a re-evaluation of  
977 processes and patterns, *Adv. Ecol. Res.*, 30, 1-67, doi:10.1016/S0065-2504(08)60016-1,  
978 1999.

979 Baker, I. T., Pihodko, L., Denning, A. S., Goulden, M., Miller, S., and Da Rocha, H. R.:  
980 Seasonal drought stress in the Amazon: reconciling models and observations, *J. Geophys.  
981 Res.-Biogeol.*, 113, G00B01, doi:10.1029/2007JG000644, 2008.

982 Ballantyne, D. M., Hribljan, J. A., Pypker, T. G., and Chimner, R. A.: Long-term water table  
983 manipulations alter peatland gaseous carbon fluxes in Northern Michigan, *Wetl. Ecol.  
984 Manag.*, 22, 35-47, doi:10.1007/s11273-013-9320-8, 2014.

985 Barr, A.G., Black, T.A., Hogg, E.H., Kljun, N., Morgenstern, K., and Nesic, Z.: Inter-annual  
986 variability in the leaf area index of a boreal aspen-hazelnut forest in relation to net  
987 ecosystem production, *Agric. For. Meteorol.* 126, 237-255,  
988 doi:10.1016/j.agrformet.2004.06.011, 2004.

989 Bond-Lamberty, B., Gower, S. T., and Ahl, D. E.: Improved simulation of poorly drained forests  
990 using Biome-BGC, *Tree Physiol.*, 27, 703-715, doi:10.1093/treephys/27.5.703, 2007.

991 Cai, T., Flanagan, L. B., and Syed, K. H.: Warmer and drier conditions stimulate respiration  
992 more than photosynthesis in a boreal peatland ecosystem: analysis of automatic chambers  
993 and eddy covariance measurements, *Plant Cell Environ.*, 33, 394-407, doi:10.1111/j.1365-  
994 3040.2009.02089.x, 2010.

995 Campbell, G. S.: A simple method for determining unsaturated conductivity from moisture  
996 retention data, *Soil Sci.*, 117, 311-314, 1974.

997 Choi, W. J., Chang, S. X., and Bhatti, J. S.: Drainage affects tree growth and C and N dynamics  
998 in a minerotrophic peatland, *Ecology*, 88, 443-453, doi:10.1890/0012-  
999 9658(2007)88[443:DATGAC]2.0.CO;2, 2007.

1000 Cronk, J. K. and Fennessy, M. S.: *Wetland plants: biology and ecology*, CRC press, 2001.

1001 Dimitrov, D. D., Grant, R. F., Lafleur, P. M., and Humphreys, E. R.: Modeling the effects of  
1002 hydrology on ecosystem respiration at Mer Bleue bog, *J. Geophys. Res.-Biogeo.*, 115,  
1003 G04043, doi:10.1029/2010JG001312, 2010a.

1004 Dimitrov, D. D., Grant, R. F., Lafleur, P. M., and Humphreys, E. R.: Modelling subsurface  
1005 hydrology of Mer Bleue bog, *Soil Sci. Soc. Am. J.*, 74, 680–694,  
1006 doi:10.2136/sssaj2009.0148, 2010b.

1007 Dimitrov, D. D., Grant, R. F., Lafleur, P. M., and Humphreys, E. R.: Modeling the effects of  
1008 hydrology on gross primary productivity and net ecosystem productivity at Mer Bleue bog,  
1009 *J. Geophys. Res.-Biogeo.*, 116, G04010, doi:10.1029/2010JG001586, 2011.

1010 Dise, N. B: Peatland response to global change, *Science*, 326, 810-811,  
1011 doi:10.1126/science.1174268, 2009.

1012 Flanagan, L. B. and Syed, K. H.: Stimulation of both photosynthesis and respiration in response  
1013 to warmer and drier conditions in a boreal peatland ecosystem, *Glob. Change Biol.*, 17,  
1014 2271-2287, doi:10.1111/j.1365-2486.2010.02378.x, 2011.

1015 Frolking, S., Roulet, N. T., Moore, T. R., Lafleur, P. M., Bubier, J. L., and Crill, P. M.:  
1016 Modelling the seasonal to annual carbon balance of Mer Bleue bog, Ontario, Canada,  
1017 Global Biogeochem. Cy., 16, 1-21, doi:10.1029/2001GB001457, 2002.

1018 Gerten, D., Schaphoff, S., Haberlandt, U., Lucht, W., and Sitch, S.: Terrestrial vegetation and  
1019 water balance-hydrological evaluation of a dynamic global vegetation model, J. Hydrol.,  
1020 286, 249-270, doi:10.1016/j.jhydrol.2003.09.029, 2004.

1021 Gorham, E: Northern peatlands: role in the carbon cycle and probable responses to climatic  
1022 warming, Ecol. Appl., 1, 182-195, doi: 10.2307/1941811, 1991.

1023 Goulden, M. L., Daube, B. C., Fan, S. M., Sutton, D. J., Bazzaz, A., Munger, J. W., and Wofsy,  
1024 S. C.: Physiological responses of a black spruce forest to weather, J. Geophys. Res.-  
1025 Atmos., 102, 28987-28996, doi:10.1029/97JD01111, 1997.

1026 Grant, R. F., Desai, A. R., and Sulman, B. N.: Modelling contrasting responses of wetland  
1027 productivity to changes in water table depth, Biogeosciences, 9, 4215-4231,  
1028 doi:10.5194/bg-9-4215-2012, 2012.

1029 Ise, T., Dunn, A. L., Wofsy, S. C., and Moorcroft, P. R.: High sensitivity of peat decomposition  
1030 to climate change through water-table feedback, Nat. Geosci., 1, 763-766,  
1031 doi:10.1038/ngeo331, 2008.

1032 Kotowska, A: The long-term effects of drainage on carbon cycling in a boreal fen, M.Sc. thesis,  
1033 Department of Integrative Biology, University of Guelph, Ontario, Canada, 75 pp., 2013.

1034 Krinner, G., Viovy, N., de Noblet-Ducoudré, N., Ogée, J., Polcher, J., Friedlingstein, P., Ciais,  
1035 P., Sitch, S., and Prentice, I. C.: A dynamic global vegetation model for studies of the

1036 coupled atmosphere-biosphere system, *Global Biogeochem. Cy.*, 19, GB1015,  
1037 doi:10.1029/2003GB002199, 2005.

1038 Kuiper, J. J., Mooij, W. M., Bragazza, L., and Robroek, B. J.: Plant functional types define  
1039 magnitude of drought response in peatland CO<sub>2</sub> exchange, *Ecology*, 95, 123-131,  
1040 doi:10.1890/13-0270.1, 2014.

1041 Lafleur, P. M., Hember, R. A., Admiral, S. W., and Roulet, N. T.: Annual and seasonal  
1042 variability in evapotranspiration and water table at a shrub-covered bog in southern  
1043 Ontario, *Canada, Hydrol. Process.*, 19, 3533-3550, 2005, doi: 10.1002/hyp.5842.

1044 Lieffers, V. J. and Rothwell, R. L.: Rooting of peatland black spruce and tamarack in relation to  
1045 depth of water table, *Can. J. Botany*, 65, 817-821, doi: 10.1139/b87-111, 1987.

1046 Limpens, J., Berendse, F., Blodau, C., Canadell, J. G., Freeman, C., Holden, J., Roulet, N.,  
1047 Rydin, H., and Schaeppman-Strub, G.: Peatlands and the carbon cycle: from local processes  
1048 to global implications – a synthesis, *Biogeosciences*, 5, 1475–1491, doi:10.5194/bg-5-  
1049 1475-2008, 2008.

1050 Lizama, H. M. and Suzuki, I.: Kinetics of sulfur and pyrite oxidation by *Thiobacillus*  
1051 thiooxidans. Competitive inhibition by increasing concentrations of cells, *Can. J.*  
1052 *Microbiol.*, 37, 182-187, doi:10.1139/m91-028, 1991.

1053 Long, K. D., Flanagan, L. B., and Cai, T.: Diurnal and seasonal variation in methane emissions  
1054 in a northern Canadian peatland measured by eddy covariance, *Glob. Change Biol.* 16,  
1055 2420-2435, doi:10.1111/j.1365-2486.2009.02083.x, 2010.

1056 Long, K. D.: Methane fluxes from a northern peatland: mechanisms controlling diurnal and  
1057 seasonal variation and the magnitude of aerobic methanogenesis, M.Sc. thesis, Department  
1058 of Biological Sciences, University of Lethbridge, Lethbridge, AB, Canada, 100 pp., 2008.

1059 Macdonald, S. E. and Lieffers, V. J.: Photosynthesis, water relations, and foliar nitrogen of *Picea*  
1060 *mariana* and *Larix laricina* from drained and undrained peatlands, *Can. J. Forest Res.*, 20,  
1061 995-1000, doi:10.1139/x90-133, 1990.

1062 Mäkiranta, P., Laiho, R., Fritze, H., Hytönen, J., Laine, J., and Minkkinen, K.: Indirect regulation  
1063 of heterotrophic peat soil respiration by water level via microbial community structure and  
1064 temperature sensitivity, *Soil Biol. Biochem.*, 41, 695-703,  
1065 doi:10.1016/j.soilbio.2009.01.004, 2009.

1066 Markham, J. H.: Variation in moss-associated nitrogen fixation in boreal forest stands, *Oecologia*  
1067 161, 353-359, doi: 10.1007/s00442-009-1391-0, 2009.

1068 Mettrop, I. S., Cusell, C., Kooijman, A. M., and Lamers, L. P.: Nutrient and carbon dynamics in  
1069 peat from rich fens and Sphagnum-fens during different gradations of drought, *Soil Biol.*  
1070 *Biochem.*, 68, 317-328, doi:10.1016/j.soilbio.2013.10.023, 2014.

1071 Mezbahuddin, M., Grant, R. F., and Hirano, T.: How hydrology determines seasonal and  
1072 interannual variations in water table depth, surface energy exchange, and water stress in a  
1073 tropical peatland: modeling versus measurements, *J. Geophys. Res.-Biogeo.*, 120, 2132-  
1074 2157, doi:10.1002/2015JG003005, 2015.

1075 Mezbahuddin, M., Grant, R. F., and Hirano, T.: Modelling effects of seasonal variation in water  
1076 table depth on net ecosystem CO<sub>2</sub> exchange of a tropical peatland, *Biogeosciences*, 11,  
1077 577-599, doi:10.5194/bg-11-577-2014, 2014.

1078 Mezbahuddin, M., Grant, R.F. and Flanagan, L.B.: Modeling hydrological controls on variations  
1079 in peat water content, water table depth, and surface energy exchange of a boreal western  
1080 Canadian fen peatland, *J. Geophys. Res.-Biogeo.*, 121, 2216-2242,  
1081 doi:10.1002/2016JG003501, 2016.

1082 Miller, S. D., Goulden, M. L., Menton, M. C., da Rocha, H. R., de Freitas, H. C., Figueira, A. M.  
1083 e. S., and de Sousa, C. A. D.: Biometric and micrometeorological measurements of tropical  
1084 forest carbon balance, *Ecol. Appl.*, 14, 114–126, doi:10.1890/02-6005, 2004.

1085 Moore, T. and Basiliko, N.: Decomposition in boreal peatlands, in: *Boreal peatland ecosystems*,  
1086 edited by: Wieder, R. K. and Vitt, D. H., Springer Science & Business Media, 125-143,  
1087 2006.

1088 Munir, T. M., Xu, B., Perkins, M., and Strack, M.: Responses of carbon dioxide flux and plant  
1089 biomass to water table drawdown in a treed peatland in northern Alberta: a climate change  
1090 perspective, *Biogeosciences*, 11, 807-820, doi:10.5194/bg-11-807-2014, 2014.

1091 Murphy, M., Laiho, R., and Moore, T. R.: Effects of water table drawdown on root production  
1092 and aboveground biomass in a boreal bog, *Ecosystems*, 12, 1268-1282,  
1093 doi:10.1007/s10021-009-9283-z, 2009.

1094 Parmentier, F. J. W., Van der Molen, M. K., de Jeu, R. A. M., Hendriks, D. M. D., and Dolman,  
1095 A. J.: CO<sub>2</sub> fluxes and evaporation on a peatland in the Netherlands appear not affected by

1096 water table fluctuations, *Agr. Forest Meteorol.*, 149, 1201-1208,  
1097 doi:10.1016/j.agrformet.2008.11.007, 2009.

1098 Peichl, M., Öquist, M., Löfvenius, M. O., Ilstedt, U., Sagerfors, J., Grelle, A., Lindroth, A., and  
1099 Nilsson, M. B.: A 12-year record reveals pre-growing season temperature and water table  
1100 level threshold effects on the net carbon dioxide exchange in a boreal fen, *Environ. Res.*  
1101 *Lett.*, 9, 055006, doi:10.1088/1748-9326/9/5/055006, 2014.

1102 Preston, M. D., Smemo, K. A., McLaughlin, J. W., and Basiliko, N.: Peatland microbial  
1103 communities and decomposition processes in the James Bay Lowlands, Canada, *Front.*  
1104 *Microbiol.*, 3, 70, doi:10.3389/fmicb.2012.00070, 2012.

1105 Richardson, A. D., Hollinger, D. Y., Burba, G. G., Davis, K. J., Flanagan, L. B., Katul, G. G.,  
1106 Munger, J. W., Ricciuto, D. M., Stoy, P. C., Suyker, A. E., Verma, S. B., and Wofsy, S. C.:  
1107 A multi-site analysis of random error in tower-based measurements of carbon and energy  
1108 fluxes, *Agr. Forest Meteorol.*, 136, 1-18, doi:10.1016/j.agrformet.2006.01.007, 2006.

1109 Rippy, J. F. and Nelson, P. V.: Cation exchange capacity and base saturation variation among  
1110 Alberta, Canada, moss peats, *HortScience*, 42, 349-352, 2007.

1111 Riutta, T., Laine, J., and Tuittila, E. S.: Sensitivity of CO<sub>2</sub> exchange of fen ecosystem  
1112 components to water level variation, *Ecosystems*, 10, 718-733, doi:10.1007/s10021-007-  
1113 9046-7, 2007.

1114 Riutta, T.: Fen ecosystem carbon gas dynamics in changing hydrological conditions, *Diss. For.*  
1115 67, Department of Forest Ecology, Faculty of Agriculture and Forestry, University of  
1116 Helsinki, 46pp., 2008.

1117 Schaefer, K., Collatz, G. J., Tans, P., Denning, A. S., Baker, I., Berry, J., Pihodko, L., Suits, N.,  
1118 and Philpott, A.: Combined simple biosphere/Carnegie-Ames-Stanford approach terrestrial  
1119 carbon cycle model, *J. Geophys. Res.-Biogeo.*, 113, G03034, doi:10.1029/2007JG000603,  
1120 2008.

1121 Schwärzel, K., Šimunek, J., van Genuchten, M. T., and Wessolek, G.: Measurement and  
1122 modeling of soil-water dynamics and evapotranspiration of drained peatland soils, *J. Plant  
1123 Nutr. Soil Sci.*, 169, 762-774, doi:10.1002/jpln.200621992, 2006.

1124 Sonnentag, O., van der Kamp, G., Barr, A. G., and Chen, J. M.: On the relationship between  
1125 water table depth and water vapour and carbon dioxide fluxes in a minerotrophic fen, *Glob.  
1126 Change Biol.*, 16, 1762–1776, doi:10.1111/j.1365-2486.2009.02032.x, 2010.

1127 St-Hilaire, F., Wu, J., Roulet, N. T., Frolking, S., Lafleur, P. M., Humphreys, E. R., and Arora,  
1128 V.: McGill wetland model: evaluation of a peatland carbon simulator developed for global  
1129 assessments, *Biogeosciences*, 7, 3517–3530, doi:10.5194/bg-7-3517- 2010, 2010.

1130 Strack, M., Waddington, J. M., Rochefort, L., and Tuittila, E. S.: Response of vegetation and net  
1131 ecosystem carbon dioxide exchange at different peatland microforms following water table  
1132 drawdown, *J. Geophys. Res.-Biogeo.*, 111, G02006, doi:10.1029/2005JG000145, 2006.

1133 Sulman, B. N., Desai, A. R., Cook, B. D., Saliendra, N., and Mackay, D. S.: Contrasting carbon  
1134 dioxide fluxes between a drying shrub wetland in Northern Wisconsin, USA, and nearby  
1135 forests, *Biogeosciences*, 6, 1115-1126, doi:10.5194/bg-6-1115-2009, 2009.

1136 Sulman, B. N., Desai, A. R., Saliendra, N. Z., Lafleur, P. M., Flanagan, L. B., Sonnentag, O.,  
1137 Mackay, D. S., Barr, A. G., and van der Kamp, G.: CO<sub>2</sub> fluxes at northern fens and bogs

1138 have opposite responses to inter-annual fluctuations in water table, *Geophys. Res. Lett.*, 37,  
1139 L19702, doi:10.1029/2010GL044018, 2010.

1140 Sulman, B. N., Desai, A. R., Schroeder, N. M., Ricciuto, D., Barr, A., Richardson, A. D.,  
1141 Flanagan, L. B., Lafleur, P. M., Tian, H., Chen, G., Grant, R. F., Poulter, B., Verbeeck, H.,  
1142 Ciais, P., Ringeval, B., Baker, I. T., Schaefer, K., Luo, Y., and Weng, E.: Impact of  
1143 hydrological variations on modeling of peatland CO<sub>2</sub> fluxes: Results from the North  
1144 American Carbon Program site synthesis, *J. Geophys. Res.-Biogeo.*, 117, G01031,  
1145 doi:10.1029/2011JG001862, 2012.

1146 Syed, K. H., Flanagan, L. B., Carlson, P. J., Glenn, A. J., and Van Gaalen, K. E.: Environmental  
1147 control of net ecosystem CO<sub>2</sub> exchange in a treed, moderately rich fen in northern Alberta,  
1148 *Agr. Forest Meteorol.*, 140, 97-114, doi:10.1016/j.agrformet.2006.03.022, 2006.

1149 Tian, H., Chen, G., Liu, M., Zhang, C., Sun, G., Lu, C., Xu, X., Ren, W., Pan, S., and Chappelka,  
1150 A.: Model estimates of net primary productivity, evapotranspiration, and water use  
1151 efficiency in the terrestrial ecosystems of the southern United States during 1895–2007,  
1152 *Forest Ecol. Manag.*, 259, 1311-1327, doi:10.1016/j.foreco.2009.10.009, 2010.

1153 Turunen, J., Tomppo, E., Tolonen, K., and Reinikainen, A.: Estimating carbon accumulation  
1154 rates of undrained mires in Finland-application to boreal and subarctic regions, *The  
1155 Holocene*, 12, 69-80, 2002.

1156 Updegraff, K., Pastor, J., Bridgman, S. D., and Johnston, C. A.: Environmental and substrate  
1157 controls over carbon and nitrogen mineralization in northern wetlands, *Ecol. Appl.*, 5, 151-  
1158 163, doi:10.2307/1942060, 1995.

1159 van Genuchten, M. T.: A closed-form equation for predicting the hydraulic conductivity of  
1160 unsaturated soils, *Soil Sci. Soc. Amer. J.*, 44, 892-898, doi:  
1161 10.2136/sssaj1980.03615995004400050002x, 1980.

1162 Waddington, J. M., Morris, P. J., Kettridge, N., Granath, G., Thompson, D. K., and Moore, P. A.:  
1163 Hydrological feedbacks in northern peatlands, *Ecohydrology*, 8, 113-127,  
1164 doi:10.1002/eco.1493, 2015.

1165 Weng, E. and Luo, Y.: Soil hydrological properties regulate grassland ecosystem responses to  
1166 multifactor global change: A modeling analysis, *J. Geophys. Res.-Biogeo.*, 113, G03003,  
1167 doi:10.1029/2007JG000539, 2008.

1168 Wesely, M. L. and Hart, R. L.: Variability of short term eddy-correlation estimates of mass  
1169 exchange, in: *The ForestAtmosphere Interaction*, edited by: Hutchinson, B. A., Hicks, B.  
1170 B., and Reidel, D., 591-612, Dordrecht, 1985.

1171 Wu, J., Kutzbach, L., Jager, D., Wille, C., and Wilmking, M.: Evapotranspiration dynamics in a  
1172 boreal peatland and its impact on the water and energy balance, *J. Geophys. Res.-Biogeo.*,  
1173 115, G04038, doi:10.1029/2009JG001075, 2010.

1174 Zhang, Y., Li, C., Trettin, C. C., Li, H., and Sun, G.: An integrated model of soil, hydrology, and  
1175 vegetation for carbon dynamics in wetland ecosystems, *Global Biogeochem. Cy.*, 16, 9-1-  
1176 9-17, doi:10.1029/2001GB001838, 2002.

1177 **Figure captions**

1178 **Fig. 1.** Schematic diagram of *ecosys* algorithms representing coupled key eco-physiological and  
1179 biogeochemical (aerobic and anaerobic) processes, and plant water relations of a typical boreal  
1180 fen peatland ecosystem that are affected by water table depth (WTD) fluctuation.  $\Psi_a$ ,  $\Psi_c$ , and  $\Psi_s$   
1181 =atmospheric, canopy and soil water potentials;  $\Psi_r$ =vascular root or non-vascular belowground  
1182 water potential;  $r_c$ =canopy stomatal resistance [=1/canopy stomatal conductance ( $g_c$ )];  $\Omega_s$ =soil  
1183 hydraulic resistance;  $\Omega_r$ =hydraulic resistance to water flow through plants; OM=organic matter;  
1184 DOC, DON, DOP=dissolved organic carbon, nitrogen, and phosphorus; POC = particulate  
1185 organic C; and POM = particulate organic matter

1186 **Fig. 2.** Layout for *ecosys* model run to represent biological, chemical and hydrological  
1187 characteristics of a Western Canadian fen peatland. Figure is not drawn to scale.  $D_{humm}$  = depth  
1188 to the bottom of a layer from the hummock surface;  $D_{holl}$  = depth to the bottom of a layer from  
1189 the hollow surface; TOC = total organic C (Flanagan and Syed, 2011); TN = total nitrogen  
1190 (Flanagan and Syed, 2011); TP = total phosphorus (Flanagan and Syed, 2011); CEC = Cation  
1191 exchange capacity (Rippy and Nelson, 2007); the value for pH was obtained from Syed et al.  
1192 (2006); WTD<sub>x</sub> = external reference water table depth representing average water table depth of  
1193 the adjacent ecosystem;  $L_t$  = distance from modelled grid cells to the adjacent watershed over  
1194 which lateral discharge / recharge occurs

1195 **Fig. 3. (a, c, e, g, i, k)** 3-day moving averages of modelled and EC-gap filled net ecosystem  
1196 productivity (NEP) (Flanagan and Syed, 2011), and **(b, d, f, h, j, l)** hourly modelled and half  
1197 hourly measured water table depth (WTD) (Syed et al., 2006; Cai et al., 2010; Long et al., 2010;  
1198 Flanagan and Syed, 2011) from 2004 to 2009 at a Western Canadian fen peatland. A positive

1199 NEP means the ecosystem is a carbon sink and a negative NEP means the ecosystem is a carbon  
1200 source. A negative WTD represents a depth below hummock/hollow surface and a positive WTD  
1201 represents a depth above hummock/hollow surface

1202 **Fig. 4.** Half hourly measured **(a)** incoming shortwave radiation, and **(b)** air temperature ( $T_a$ ); and  
1203 **(c)** hourly modelled and half hourly measured water table depth (WTD) (Syed et al., 2006; Cai et  
1204 al.; 2010, Long et al.; 2010, Flanagan and Syed, 2011) during August of 2005, 2006 and 2008 at  
1205 a Western Canadian fen peatland. A negative WTD represents a depth below hummock/hollow  
1206 surface and a positive WTD represents a depth above hummock/hollow surface. Grey arrows  
1207 indicate nights with similar temperatures

1208 **Fig. 5. (a)** Half hourly EC-gap filled (Flanagan and Syed, 2011) and hourly modelled ecosystem  
1209 net  $\text{CO}_2$  fluxes, **(b)** half hourly automated chamber measured (Cai et al., 2010) and hourly  
1210 modelled understorey and soil  $\text{CO}_2$  fluxes, and **(c)** hourly modelled soil  $\text{CO}_2$  and  $\text{O}_2$  fluxes  
1211 during August of 2005, 2006 and 2008 at a Western Canadian fen peatland. No chamber  $\text{CO}_2$   
1212 flux measurement was available for 2008. Bars represent standard errors of means of chamber  
1213  $\text{CO}_2$  fluxes ( $n=9$ ). A negative flux represents an upward flux or a flux out of the ecosystem and a  
1214 positive flux represents a downward flux or a flux into the ecosystem. Grey arrows indicate  
1215 nights with similar temperatures (Fig. 4)

1216 **Fig. 6. (a-c)** Half hourly observed air temperature ( $T_a$ ), **(d-f)** hourly modelled and half hourly  
1217 observed water table depth (WTD) (Syed et al., 2006; Cai et al., 2010; Long et al., 2010;  
1218 Flanagan and Syed, 2011), **(g-i)** half hourly EC-gap filled (Flanagan and Syed, 2011) and hourly  
1219 modelled ecosystem net  $\text{CO}_2$  fluxes, **(j-l)** half hourly automated chamber measured (Cai et al.,  
1220 2010) and hourly modelled understorey and soil  $\text{CO}_2$  fluxes during July-August of 2005, 2006

1221 and 2008 at a Western Canadian fen peatland. No chamber CO<sub>2</sub> flux measurement was available  
1222 for 2008. Bars represent standard errors of means of chamber CO<sub>2</sub> fluxes ( $n=9$ ). A negative flux  
1223 represents an upward flux or a flux out of the ecosystem and a positive flux represents a  
1224 downward flux or a flux into the ecosystem. A negative WTD represents a depth below  
1225 hummock/hollow surface and a positive WTD represents a depth above hummock/hollow  
1226 surface

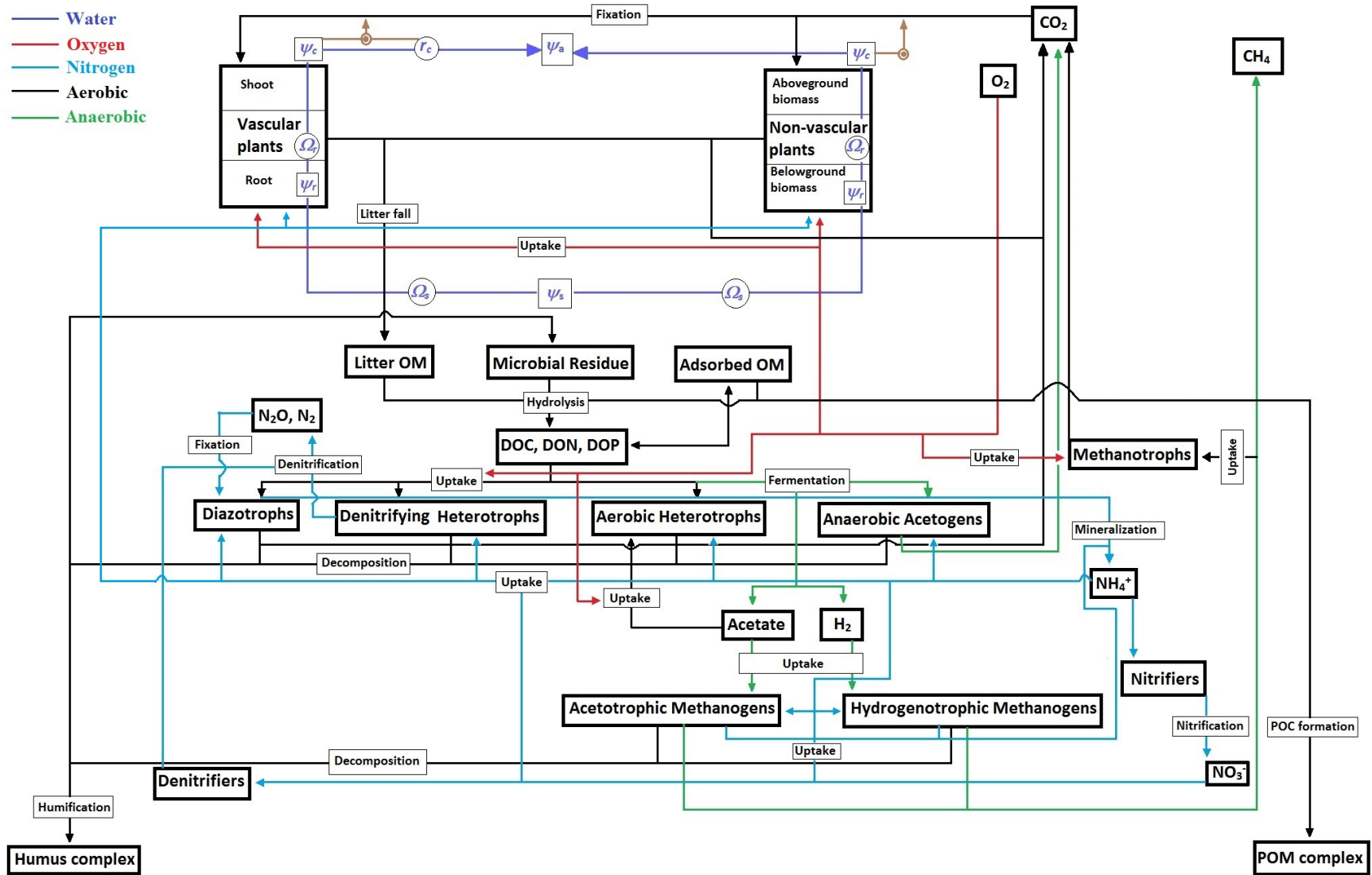
1227 **Fig. 7.** Modelled and EC-derived (Flanagan and Syed, 2011) growing season (May-August)  
1228 sums of **(a)** net ecosystem productivity (NEP), **(b)** gross primary productivity (GPP), and **(c)**  
1229 ecosystem respiration ( $R_e$ ) during 2004-2009; **(d)** observed mean growing season air temperature  
1230 ( $T_a$ ) and measured and modelled average growing season water table depth (WTD) during 2004-  
1231 2009; Modelled and EC-derived (Flanagan and Syed, 2011) annual sums of **(e)** NEP, **(f)** GPP,  
1232 and **(g)**  $R_e$  during 2004-2008; and **(h)** observed mean annual  $T_a$  and measured and modelled  
1233 average WTD during ice free periods (May-October) of 2004-2008 at a Western Canadian fen  
1234 peatland. A negative WTD represents a depth below hollow surface and a positive WTD  
1235 represents a depth above hollow surface. A positive NEP means the ecosystem is a carbon sink.  
1236 Annual modelled vs. EC-gap filled NEP, GPP,  $R_e$  estimates for 2009 were not compared due to  
1237 the lack of flux measurements from September to December in that year.

1238 **Fig. 8.** Regressions ( $P<0.001$ ) of growing season (May-August) sums of modelled and EC-  
1239 derived (Flanagan and Syed, 2011) **(a)** net ecosystem productivity (NEP), **(b)** gross primary  
1240 productivity (GPP), and **(c)** ecosystem respiration ( $R_e$ ) on growing season averages of modelled  
1241 and observed water table depth (WTD) during 2004-2009; and regressions ( $P<0.001$ ) of annual  
1242 sums of modelled and EC-derived (Flanagan and Syed, 2011) **(d)** NEP, **(e)** GPP and **(f)**  $R_e$  on  
1243 average modelled and measured WTD during ice free periods (May-October) of 2004-2008 at a

1244 Western Canadian fen peatland. A negative WTD represents a depth below hollow surface and a  
1245 positive WTD represents a depth above hollow surface. A positive NEP means the ecosystem is  
1246 a carbon sink

1247 **Fig. 9.** (a) Observed, simulated (real-time simulation) and projected (drainage simulation)  
1248 average growing season (May-August) water table depth (WTD); EC-derived, simulated and  
1249 projected growing season sums of (b) net ecosystem productivity (NEP), (c) gross primary  
1250 productivity (GPP), and (d) ecosystem respiration ( $R_e$ ); and regressions ( $P<0.001$ ) of simulated  
1251 and projected sums of (e) NEP, (f) GPP, and (g)  $R_e$  on simulated and projected average growing  
1252 season WTD during 2004-2009 at a Western Canadian fen peatland. A negative WTD represents  
1253 a depth below hollow surface and a positive WTD represents a depth above hollow surface. A  
1254 positive NEP means the ecosystem is a C sink

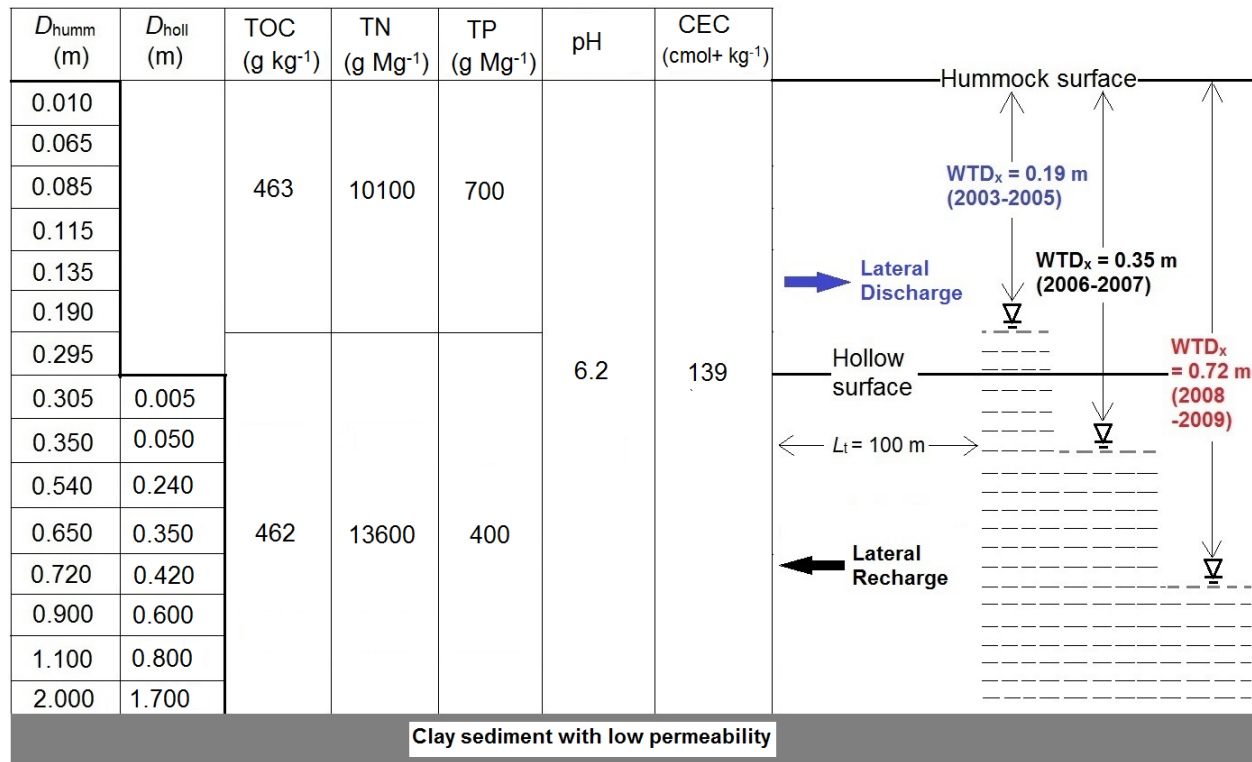
1255 **Fig. 10.** Simulated (real-time simulation) and projected (drainage simulation) (a) average  
1256 growing season (May-August) water table depth (WTD), (b) growing season sums of non-  
1257 vascular (moss) gross primary productivity (GPP), and (c) growing season sums of vascular  
1258 GPP; and regressions ( $P<0.001$ ) of simulated and projected sums of (d) non-vascular GPP, and  
1259 (e) vascular GPP on simulated and projected average growing season WTD during 2004-2009 at  
1260 a Western Canadian fen peatland. A negative WTD represents a depth below hollow surface and  
1261 a positive WTD represents a depth above hollow surface

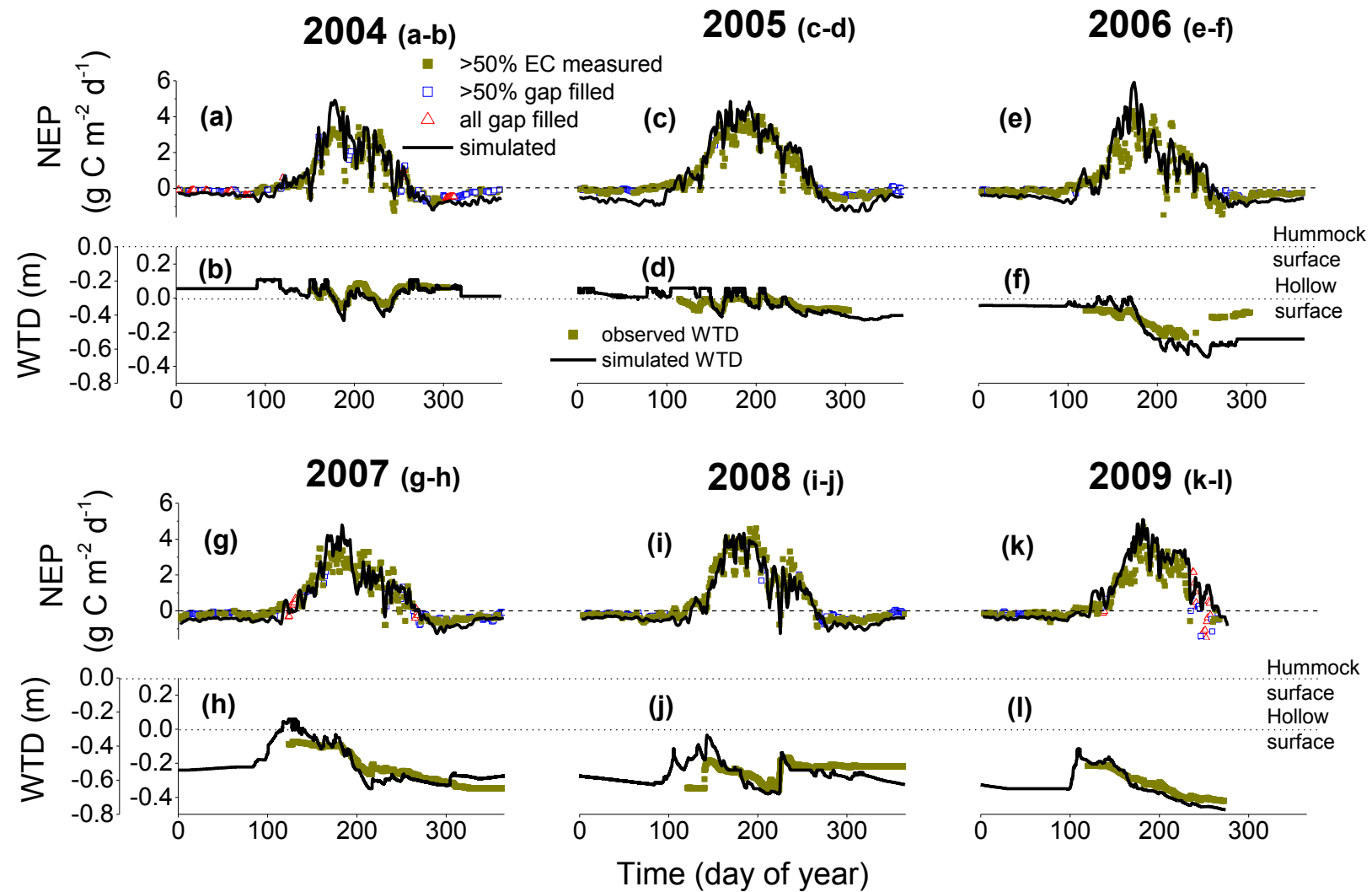


1262

1263 **Fig. 1.**

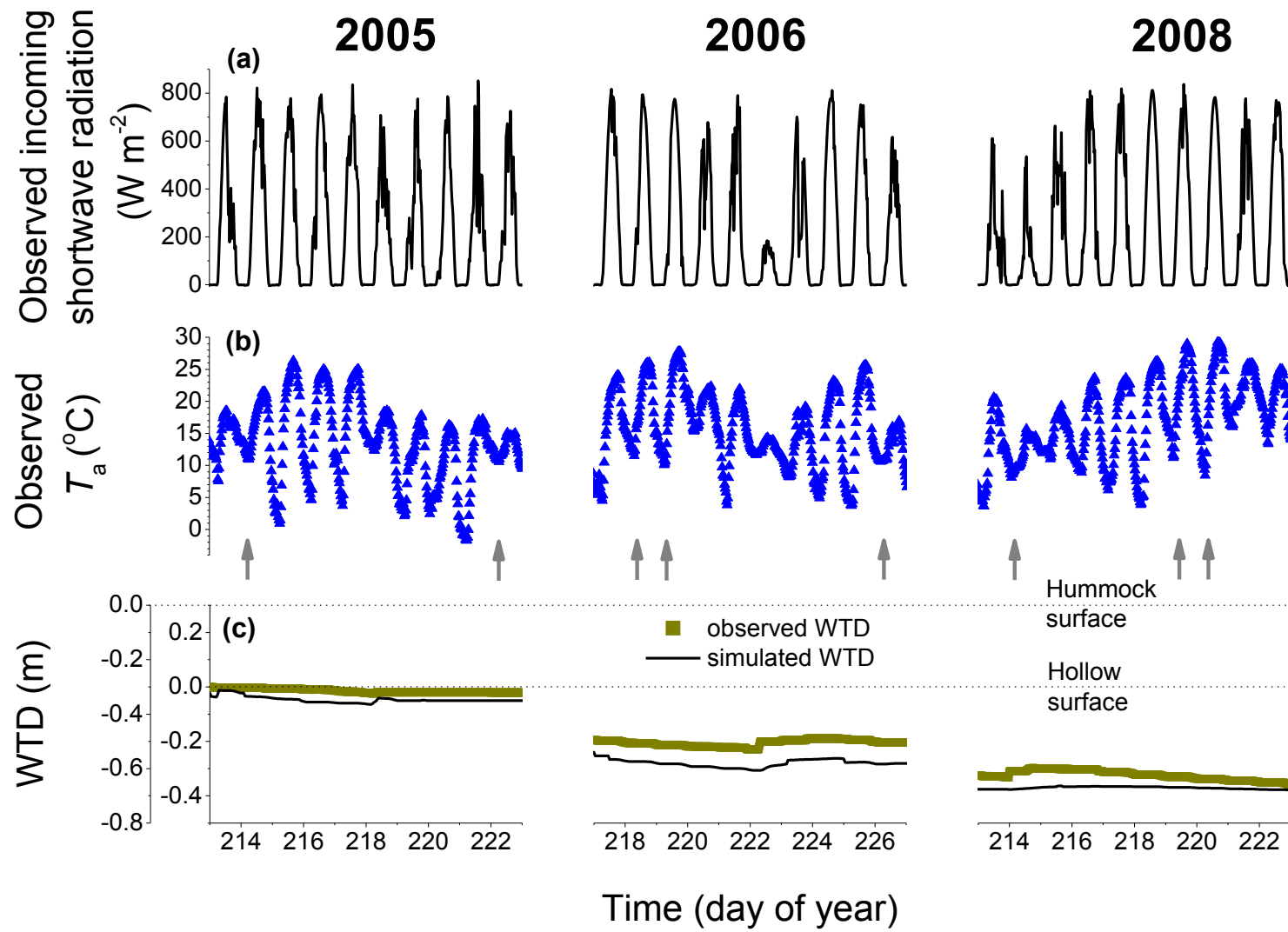
62

1266 **Fig. 2.**



1267

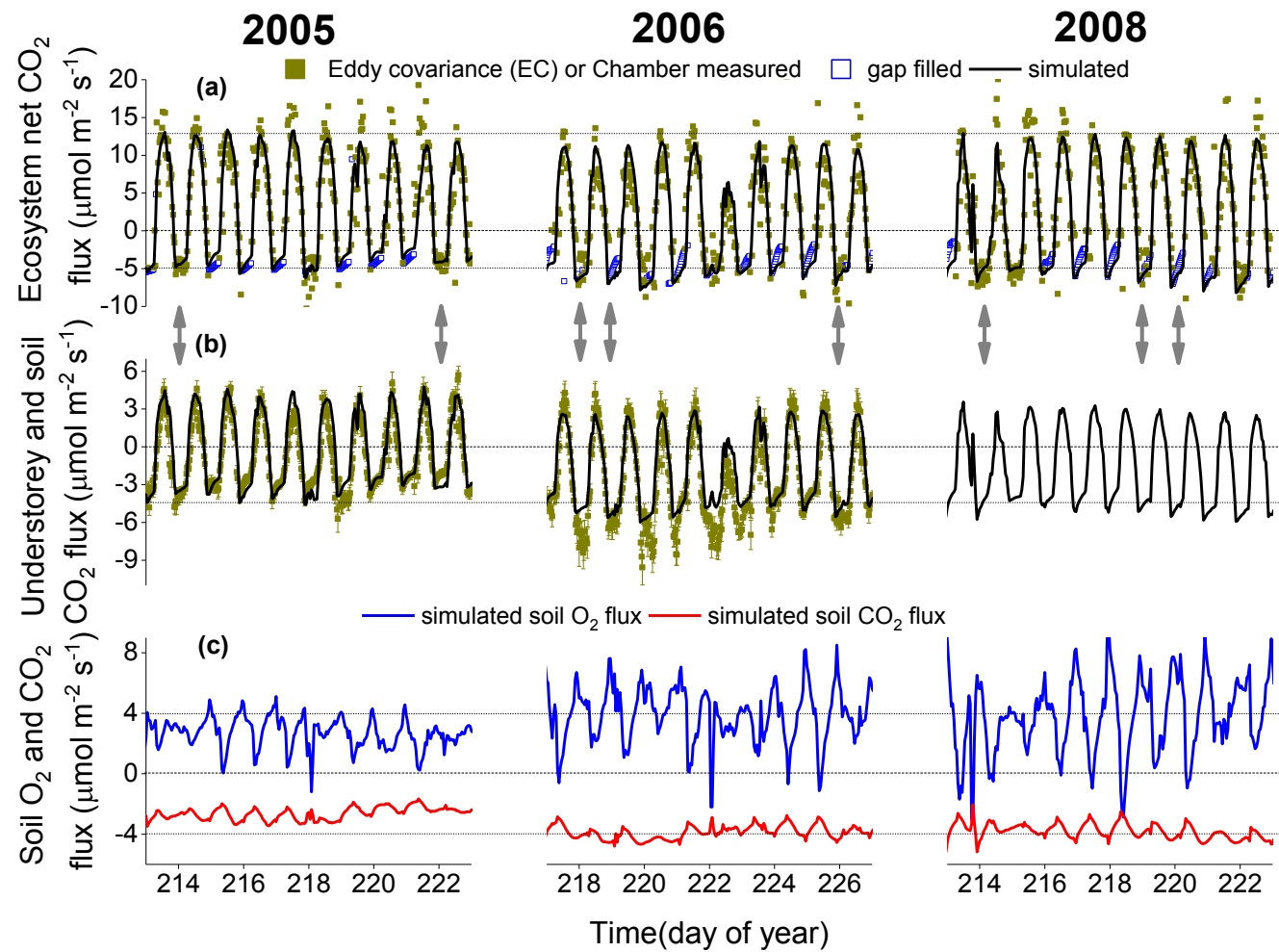
1268 Fig. 3.



1269

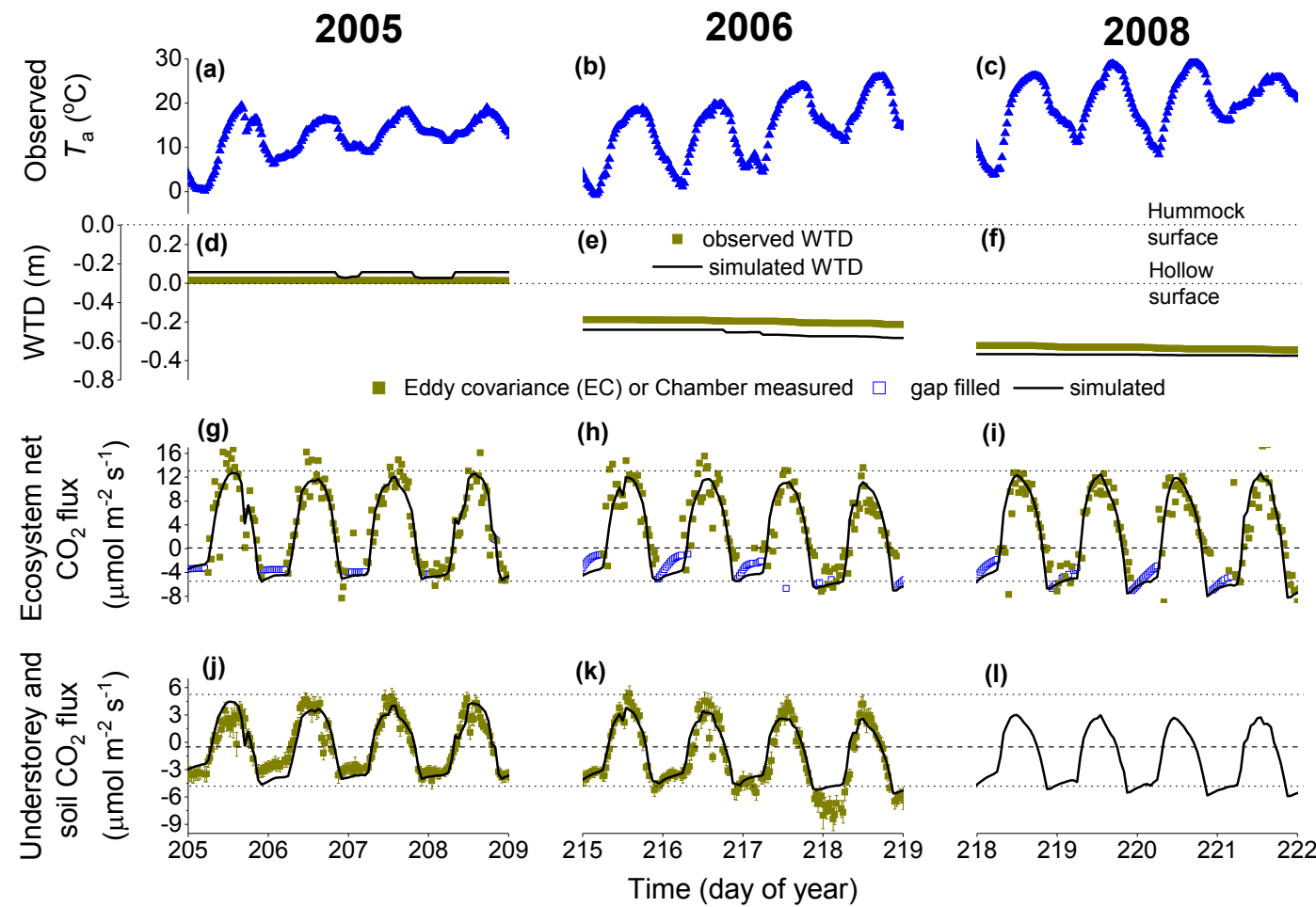
1270 **Fig. 4.**

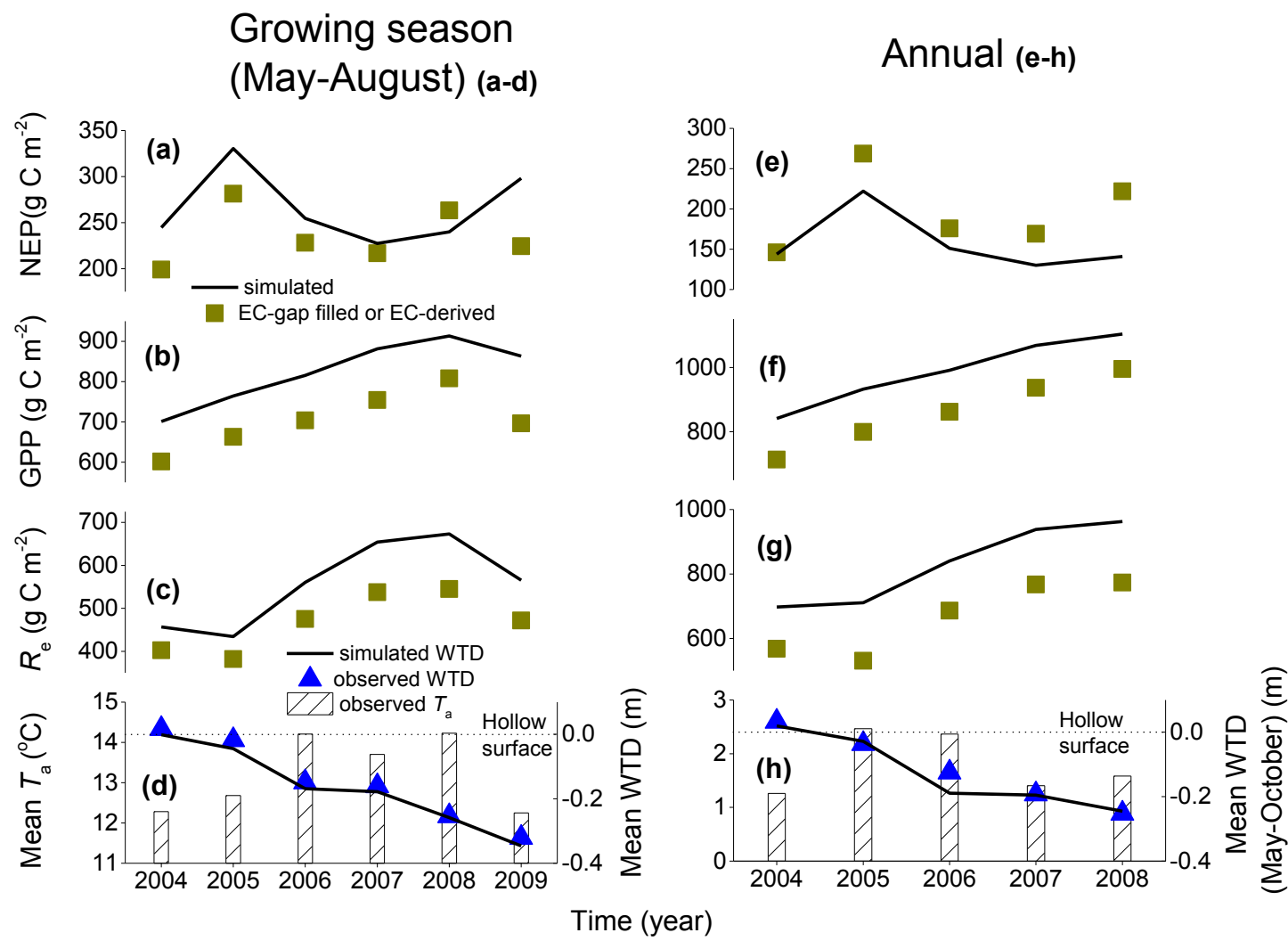
1271



1272

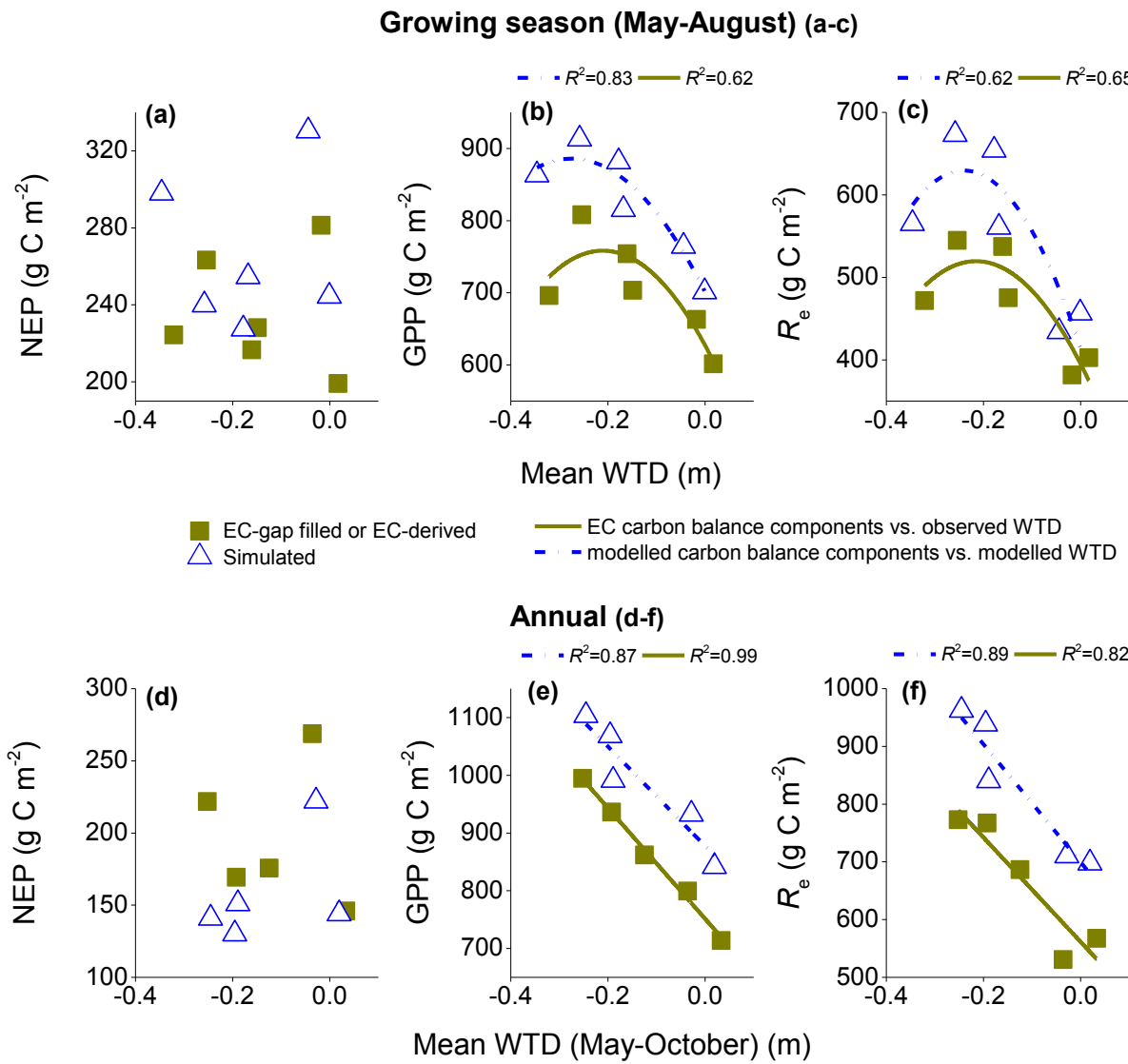
1273 **Fig. 5.**

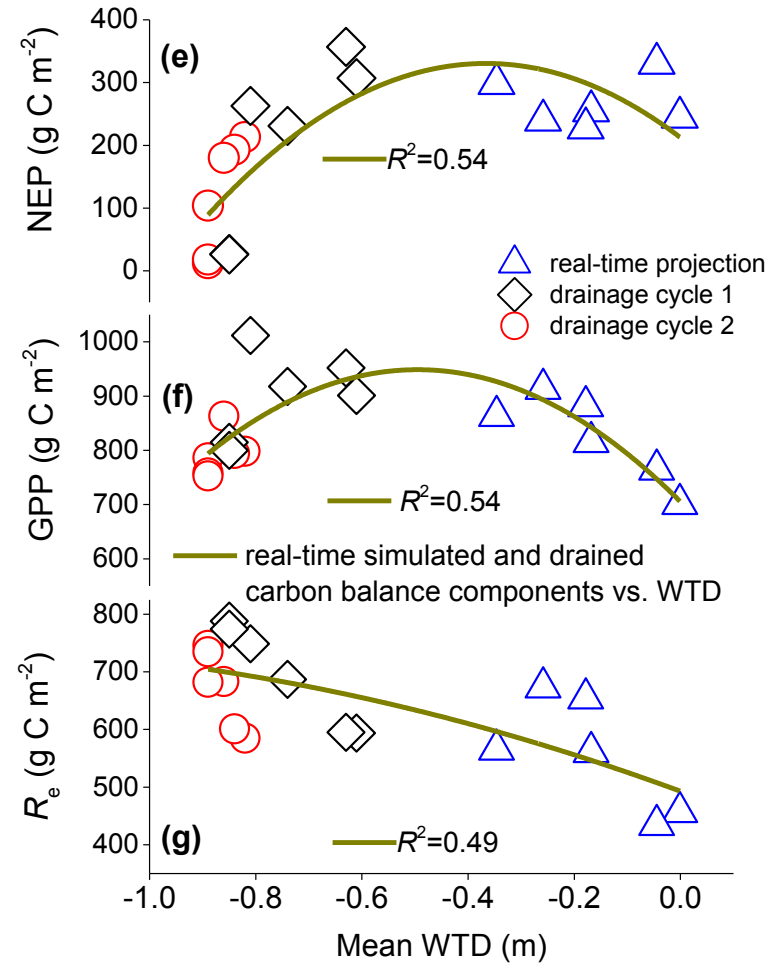
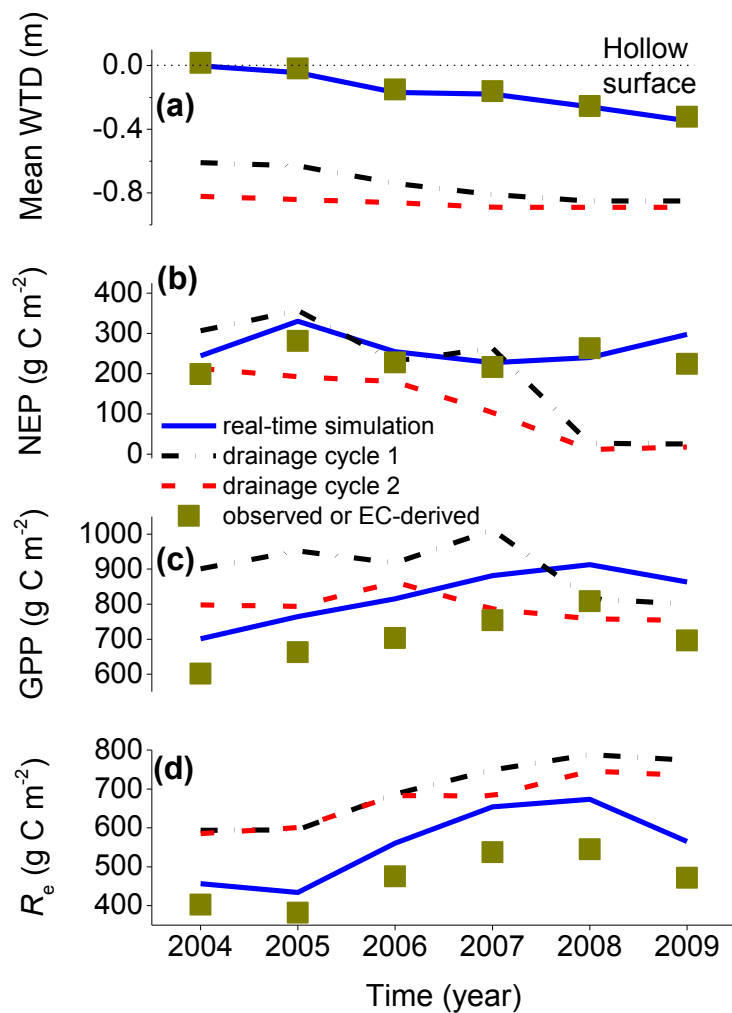




1277

1278 **Fig. 7.**





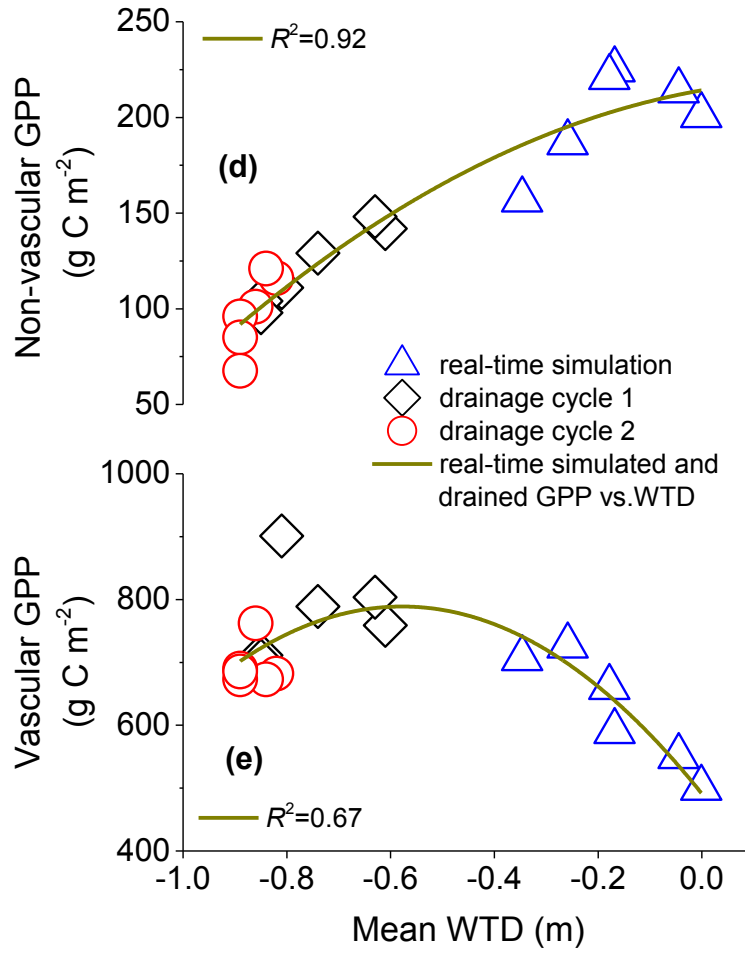
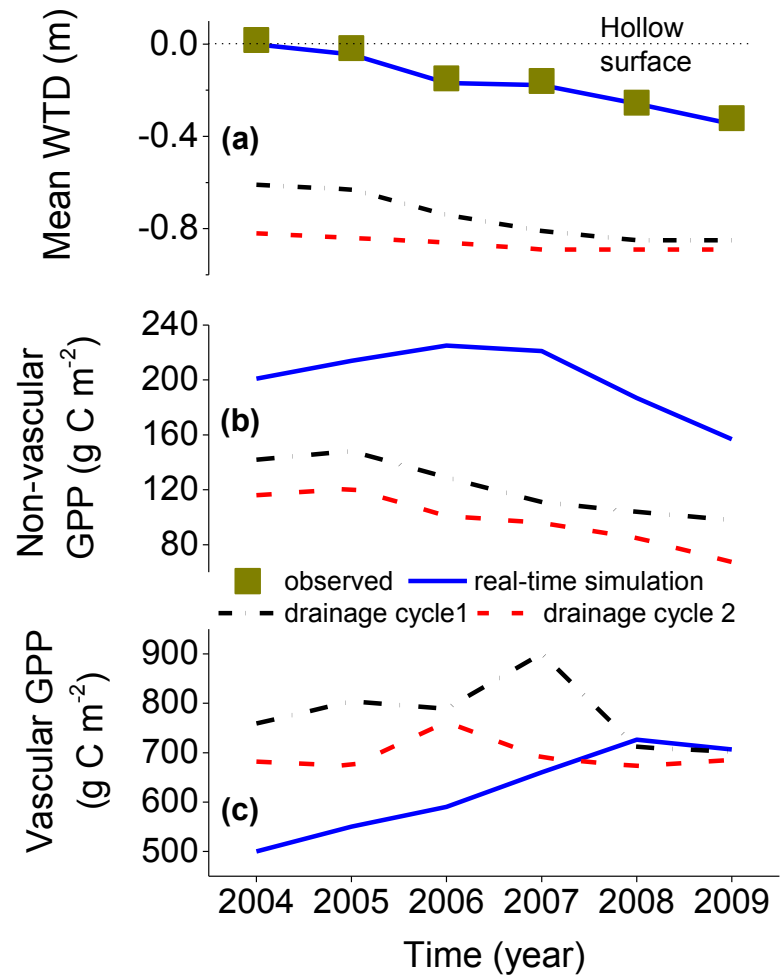


**Table 1.** Statistics from regressions between hourly modelled and measured net CO<sub>2</sub> fluxes from 2004-2009 at a Western Canadian fen peatland

| <b>(a)</b> Regressions of modelled vs. EC measured (recorded at $u^* > 0.15 \text{ m s}^{-1}$ ) net ecosystem CO <sub>2</sub> fluxes over whole years of 2004-2008 <sup>a</sup>              |  |      |            |           |                |  |   |
|--|--|------|------------|-----------|----------------|--|---|
| Year   | Total annual precipitation<br>(mm)         | n    | a          | b         | R <sup>2</sup> | RMSE<br>( $\mu\text{mol m}^{-2} \text{s}^{-1}$ ) | RMSRE<br>( $\mu\text{mol m}^{-2} \text{s}^{-1}$ ) |
| 2004   | 553  | 5034 | 0.08±0.03  | 1.10±0.01 | 0.81           | 1.58   | 1.92  |
| 2005   | 387  | 5953 | 0.07±0.03  | 1.03±0.01 | 0.82           | 1.68   | 1.99  |
| 2006   | 465  | 6012 | 0.07±0.03  | 1.08±0.01 | 0.79           | 1.68   | 1.98  |
| 2007   | 431  | 5385 | 0.06±0.03  | 0.99±0.01 | 0.79           | 1.83   | 2.09  |
| 2008   | 494  | 5843 | -0.01±0.02 | 0.98±0.01 | 0.84           | 1.63   | 2.02  |
| <b>(b)</b> Regressions of modelled vs. EC measured (recorded at $u^* > 0.15 \text{ m s}^{-1}$ ) net ecosystem CO <sub>2</sub> fluxes over growing seasons (May-August) of 2004-2009          |  |      |            |           |                |  |   |
| Year   | Total growing season precipitation<br>(mm) | n    | a          | b         | R <sup>2</sup> | RMSE<br>( $\mu\text{mol m}^{-2} \text{s}^{-1}$ ) | RMSRE<br>( $\mu\text{mol m}^{-2} \text{s}^{-1}$ ) |
| 2004   | 287  | 2043 | 0.55±0.07  | 1.05±0.01 | 0.78           | 2.27   | 2.55  |
| 2005   | 276  | 2200 | 0.82±0.07  | 0.98±0.01 | 0.79           | 2.50   | 2.74  |
| 2006   | 253  | 2107 | 0.48±0.07  | 1.06±0.01 | 0.78           | 2.36   | 2.76  |
| 2007   | 237  | 1822 | 0.65±0.07  | 0.93±0.01 | 0.75           | 2.91   | 3.06  |
| 2008   | 276  | 2070 | 0.32±0.07  | 0.96±0.01 | 0.82           | 2.45   | 2.85  |
| 2009   | 138  | 1870 | 0.76±0.08  | 1.01±0.01 | 0.81           | 2.27   | 2.83  |
| <b>(c)</b> Regressions of modelled vs. measured chamber net CO <sub>2</sub> fluxes (understorey vegetation and soil CO <sub>2</sub> fluxes) over ice free periods (May-October) of 2005-2006 |  |      |            |           |                |  |   |

| Year | Mean May-October WTD (m) |           | <i>n</i> | <i>a</i>  | <i>b</i>  | <i>R</i> <sup>2</sup> | RMSE (μmol m <sup>-2</sup> s <sup>-1</sup> ) | RMSRE (μmol m <sup>-2</sup> s <sup>-1</sup> ) |
|------|--------------------------|-----------|----------|-----------|-----------|-----------------------|--|---|
|      | Mod-elled                | Meas-ured |          |           |           |                       |  |   |
| 2005 | 0.33                     | 0.34      | 3285     | 0.43±0.02 | 1.05±0.01 | 0.68                  | 1.19   | 2.38  |
| 2006 | 0.48                     | 0.42      | 3855     | 0.31±0.03 | 0.85±0.01 | 0.71                  | 1.44   | 3.25  |

WTD = water table depth below the hummock surface; (*a*, *b*) from simple linear regressions of modelled on measured (± standard errors), and *R*<sup>2</sup> = coefficient of determination; RMSE = root mean square for errors from simple linear regressions of measured on simulated; RMSRE = root mean square for random errors in measurements; RMSRE for eddy covariance (EC) measurements were estimated by inputting EC CO<sub>2</sub> fluxes recorded at *u*\* (friction velocity) > 0.15 m s<sup>-1</sup> into algorithms for estimation of random errors due to EC CO<sub>2</sub> measurements developed for forests by Richardson et al. (2006); <sup>a</sup> whole year modelled vs. EC net CO<sub>2</sub> flux regression for 2009 could not be done due to the lack of flux measurements from September to December in that year.

**Table 2.** Effects of water table depth (WTD) drawdown on components of ecosystem carbon and nutrient cycles of a Western Canadian fen peatland

|  | Modelled   | Eddy covariance-derived/biometrically measured at the site <sup>a</sup>   | Values from other studies in similar peatlands   |
|--|--|---|--|
| Growing season (May to August) mean WTD drawdown from 2004 to 2009     | from 0.3 m below the hummock surface (at the hollow surface) in 2004 to 0.65 m below the hummock surface (0.35 below the hollow surface) in 2009 | from 0.32 m below the hummock surface (0.02 m below the hollow surface) in 2004 to 0.62 m below the hummock surface (0.32 m below the hollow surface) in 2009 |  |
| Rate of increase in annual $R_e$ with each 0.1 m of WTD drawdown       | 0.26 $\mu\text{mol CO}_2 \text{ m}^{-2} \text{ s}^{-1}$  | 0.16 $\mu\text{mol CO}_2 \text{ m}^{-2} \text{ s}^{-1}$   | 0.32±0.27 $\mu\text{mol CO}_2 \text{ m}^{-2} \text{ s}^{-1}$ <sup>b</sup>  |
| Rate of increase in growing season GPP with each 0.1 m of WTD drawdown | 0.39 $\mu\text{mol CO}_2 \text{ m}^{-2} \text{ s}^{-1}$  | 0.22 $\mu\text{mol CO}_2 \text{ m}^{-2} \text{ s}^{-1}$   | (1) 0.32±0.15 $\mu\text{mol CO}_2 \text{ m}^{-2} \text{ s}^{-1}$ <sup>b</sup><br>(2) 0.47±0.06 $\mu\text{mol CO}_2 \text{ m}^{-2} \text{ s}^{-1}$ <sup>c</sup> |
| Black Spruce   | 14.3 $\text{g N kg}^{-1} \text{ C}$  | 12.4±0.6 $\text{g N kg}^{-1} \text{ C}$   |  |

|  |              |  |  |
|--|--------------|--|--|
| Leaf nitrogen concentration (mid-July 2004)                  | Tamarack     | 32.1 g N kg <sup>-1</sup> C  | 32.6±1.4 g N kg <sup>-1</sup> C  |
|  | Dwarf Birch  | 37.4 g N kg <sup>-1</sup> C  | 41.4±1.8 g N kg <sup>-1</sup> C  |
| Leaf nitrogen (N) to phosphorus (P) ratio (mid-July 2004)    | Black Spruce | 6.6:1  | 7.1:1  |
|  | Tamarack     | 5.2:1  | 6.3:1  |
|  | Dwarf Birch  | 4.8:1  |  |
| Increase in foliar nitrogen concentrations with WTD drawdown | Black Spruce | from 14.3 to 17.2 g N kg <sup>-1</sup> C with the growing season WTD drawdown from 0.3 m below the hummock surface in 2004 to 0.65 m below the hummock surface in 2009 | (1) from 20.8±0.6 to 27±0.4 g N kg <sup>-1</sup> C with a WTD drawdown from 0.24 to 0.7 m below peat surface <sup>d</sup><br><br>(2) from 18.7±0.05 to 21.3±0.06 g N kg <sup>-1</sup> C for a WTD drawdown by 0.4-0.5 m <sup>e</sup> |
|  | Tamarack     | from 32.1 to 36.7 g N kg <sup>-1</sup> C with the growing season WTD drawdown from 0.3 m below the hummock surface in 2004 to 0.65 m below the hummock surface in 2009 | (1) from 41.4±0.4 to 66.2±1.2 g N kg <sup>-1</sup> C for a WTD drawdown from 0.24 to 0.7 m below peat surface <sup>d</sup><br><br>(2) from 35.9±0.1 to 41.7±0.18 g N kg <sup>-1</sup> C for a WTD drawdown by 0.4-0.5 m <sup>e</sup> |
|  | Dwarf Birch  | from 37.4 to 45.1 g N kg <sup>-1</sup> C with the growing season WTD drawdown from 0.3 m below the hummock surface in 2004 to 0.65                                     |  |

| m below the hummock surface in 2009                 |              |   |  |
|---|--------------|---|--|
| Increase in maximum rooting depth with WTD drawdown | Black spruce | from 0.35 to 0.65 m below the hummock surface with the growing season WTD drawdown from 0.3 m below the hummock surface in 2004 to 0.65 m below the hummock surface in 2009 | from 0.1 to 0.6 m below hummock surface with a WTD drawdown from 0.1 to 0.7 m below hummock surface <sup>f</sup> |
|   | Tamarack     | from 0.35 to 0.65 m below the hummock surface with the growing season WTD drawdown from 0.3 m below the hummock surface in 2004 to 0.65 m below the hummock surface in 2009 | from 0.2 to 0.6 m below hummock surface with a WTD drawdown from 0.1 to 0.6 m below hummock surface <sup>f</sup> |

GPP=gross primary productivity;  $R_e$  = ecosystem respiration; <sup>a</sup> Syed et al. (2006), Flanagan and Syed (2011); <sup>b</sup> Peichl et al. (2012) for a Swedish fen; <sup>c</sup> Ballantyne et al. (2014) for a Michigan fen peatland complex that has similar peat and plant functional types as our study site; <sup>d</sup> Choi et al. (2007) for a central Alberta fen peatland located ~350 km to the southwest of the study site; <sup>e</sup> Macdonald and Lieffers (1990) for a northern Alberta fen peatland located ~250 km to the northwest of the study site; <sup>f</sup> Lieffers and Rothwell (1987) for a northern Alberta fen peatland located ~250 km to the northwest of the study site

